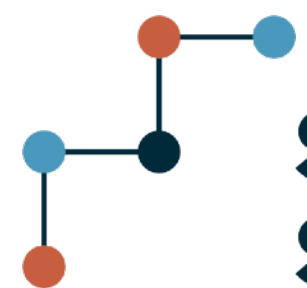


Delensing the Cosmic Microwave Background

Julien Carron, Berkeley RPM seminar, October 22 2024

(S. Belkner, L. Legrand, M. Robertson, A. Lewis, G. Fabbian, R. Durrer, E. Di Dio, CMB-S4, ...)



**Swiss National
Science Foundation**

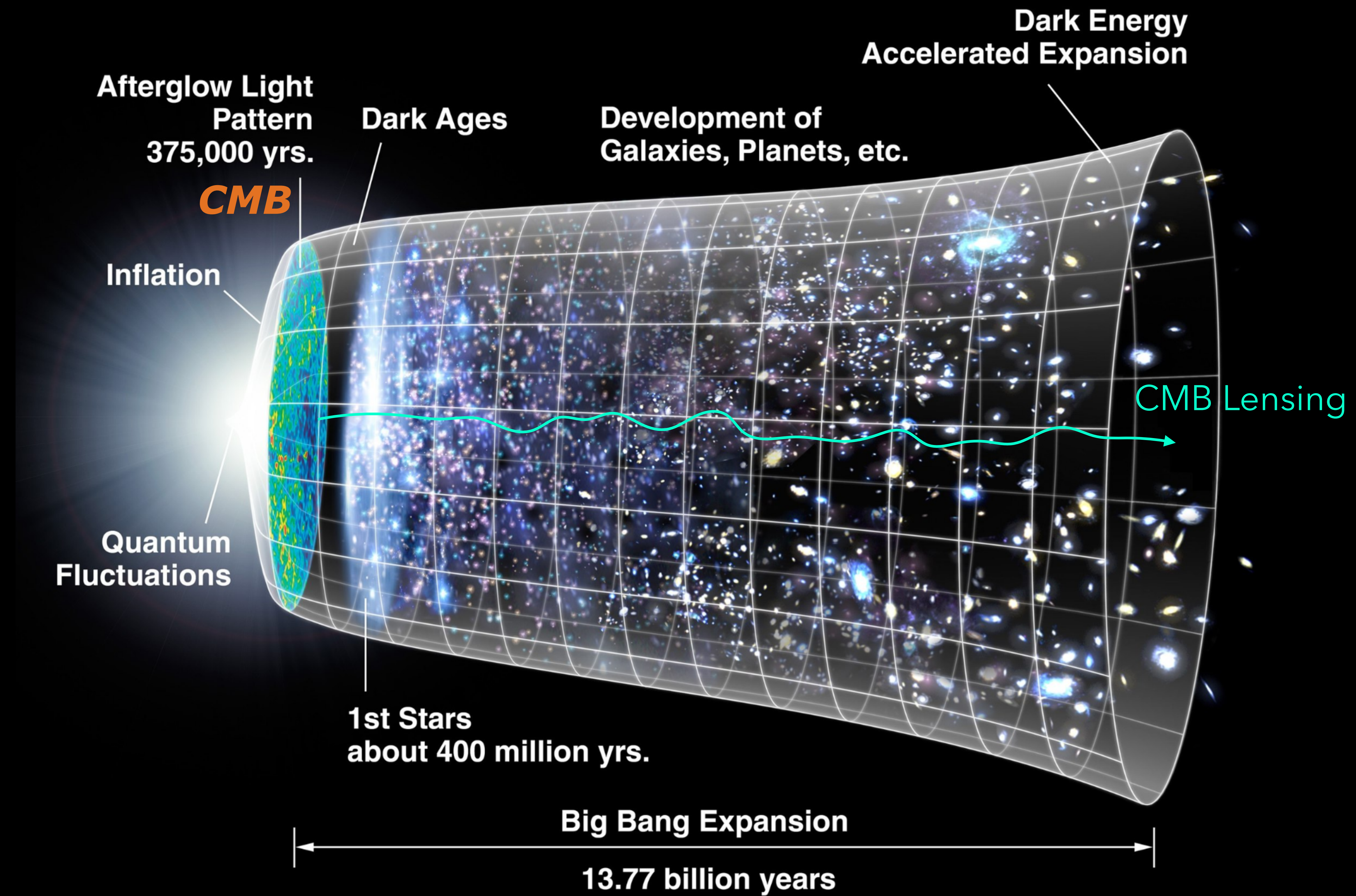


**UNIVERSITÉ
DE GENÈVE**

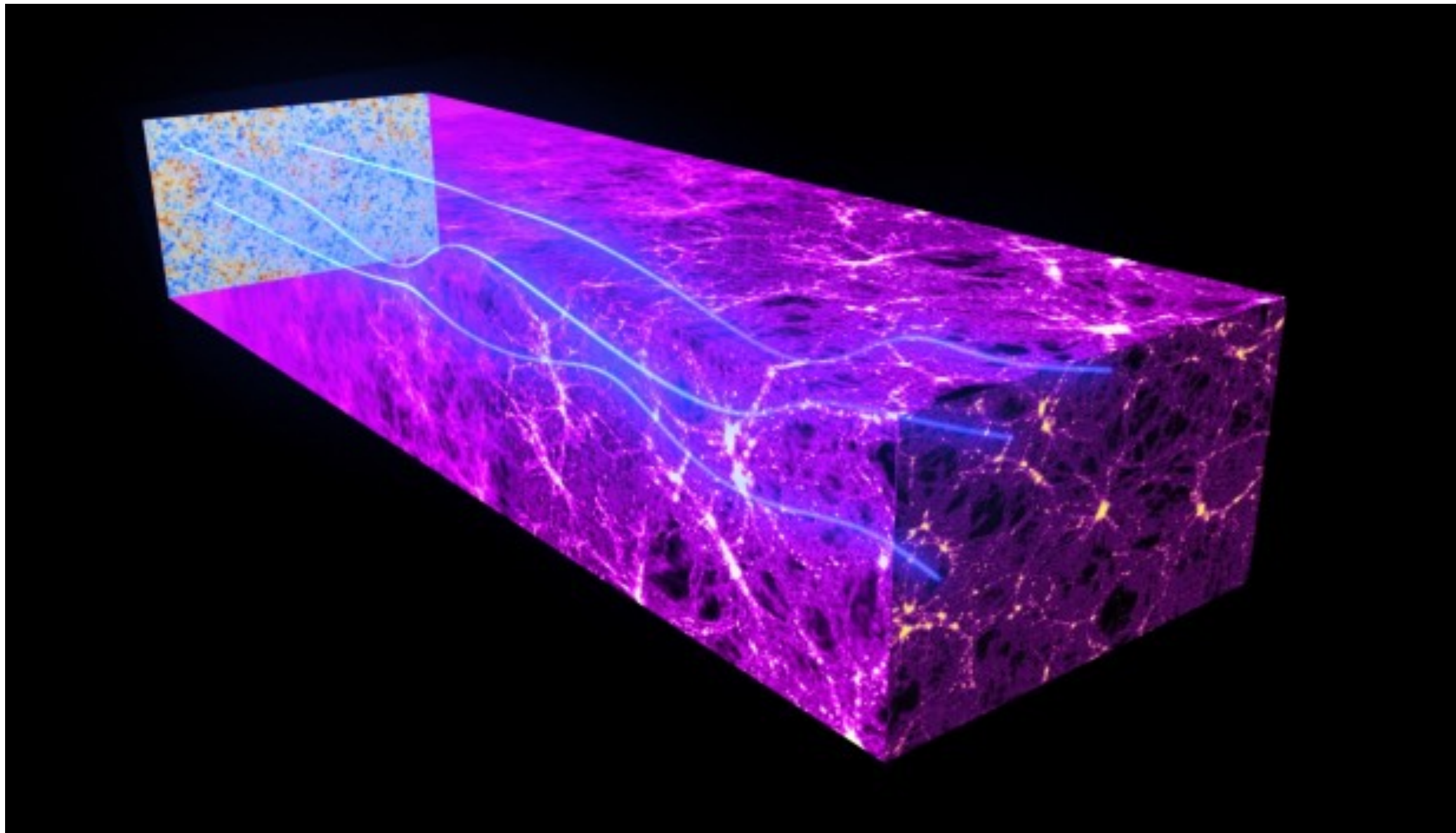
Outline

- Intro to CMB lensing and delensing
- Lensing from deep polarization experiments – « EB » estimators
- Likelihood-based (« Bayesian ») lensing map estimation / delensing, CMB-S4 delensing.

Belkner et al 2024 (for CMB-S4)



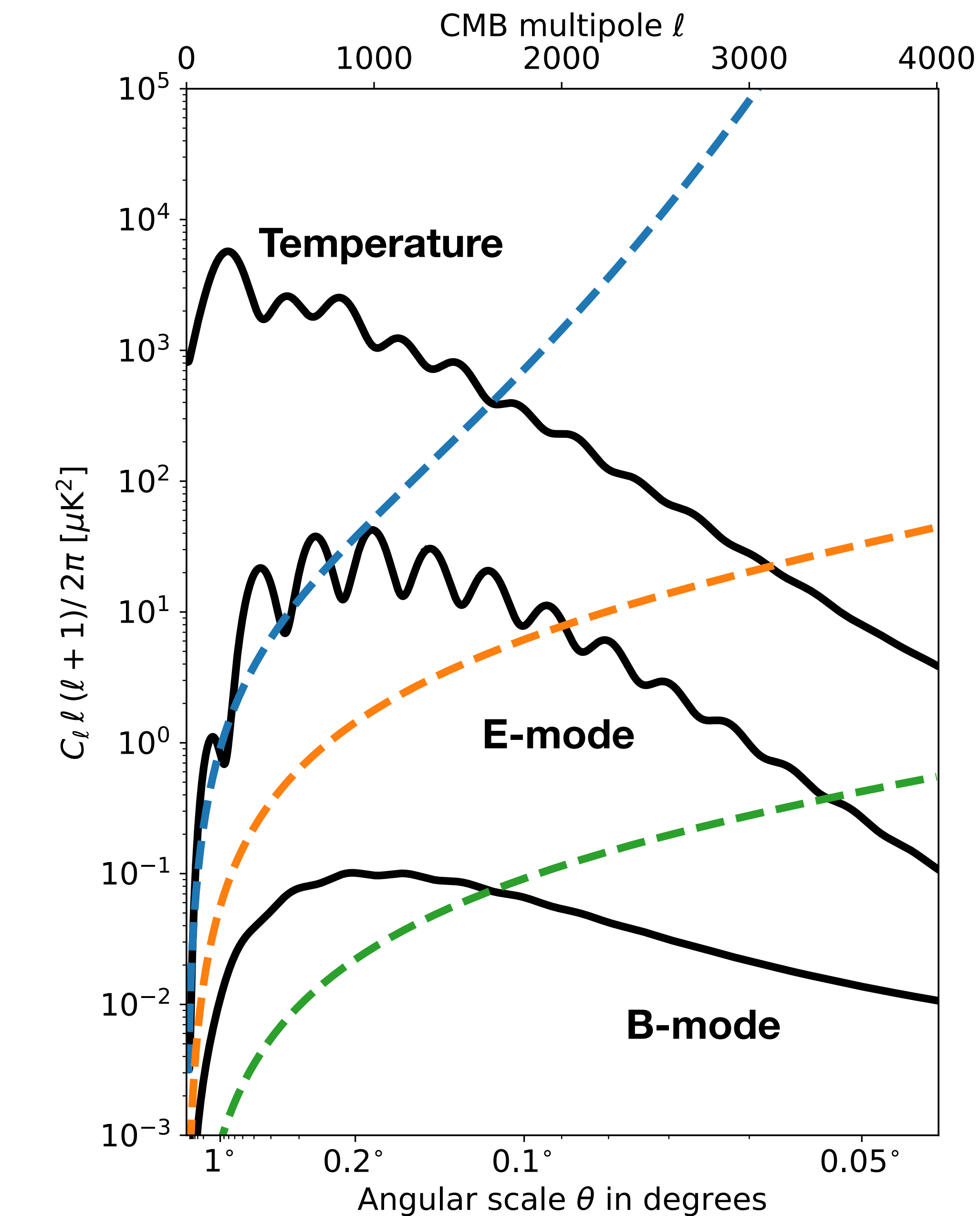
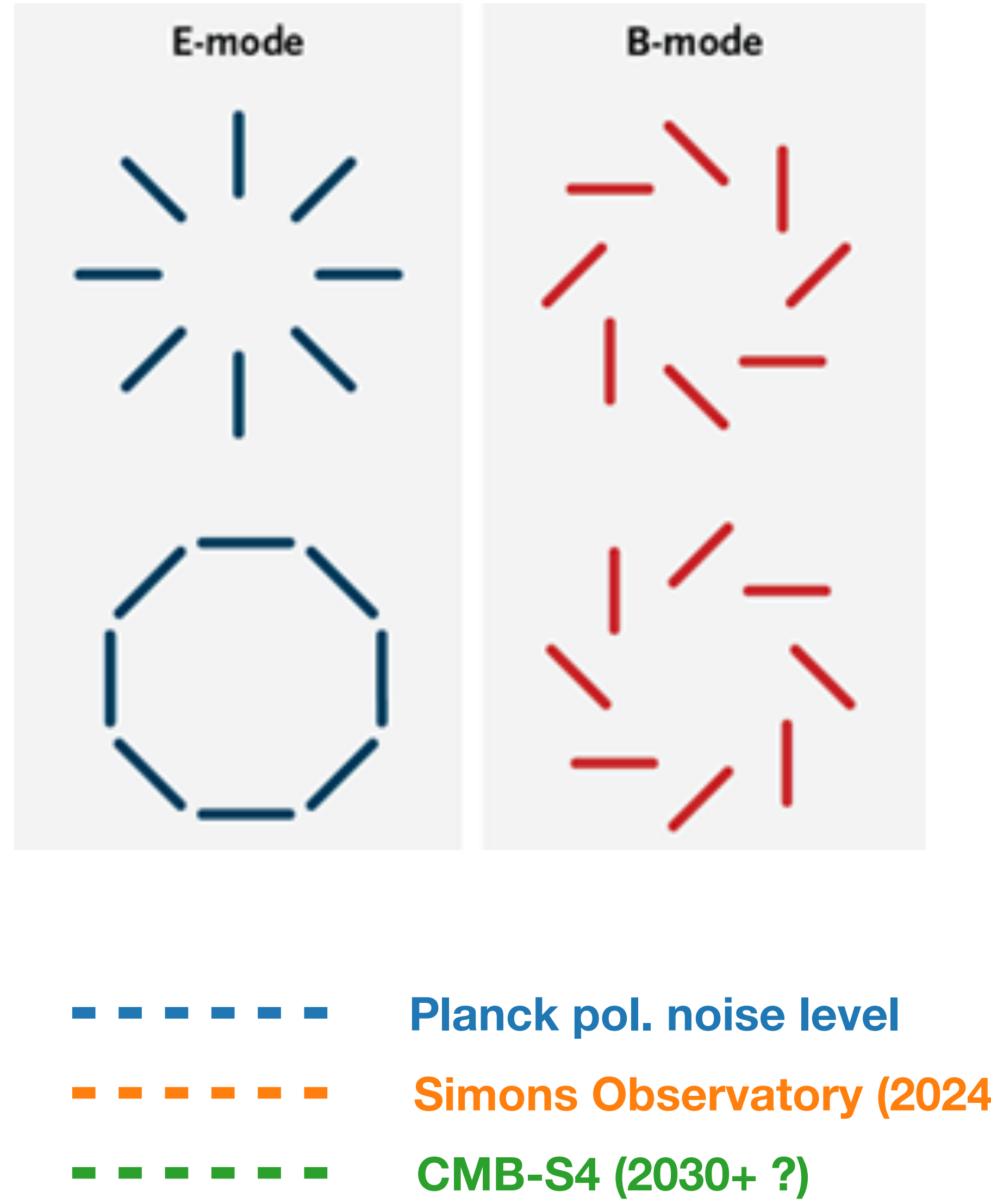
CMB Lensing

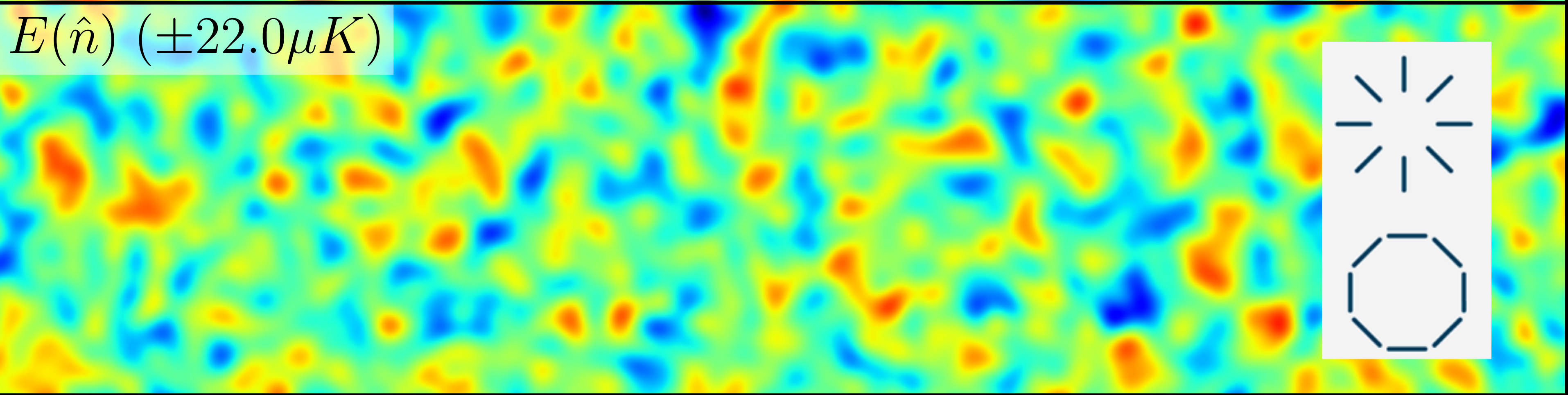
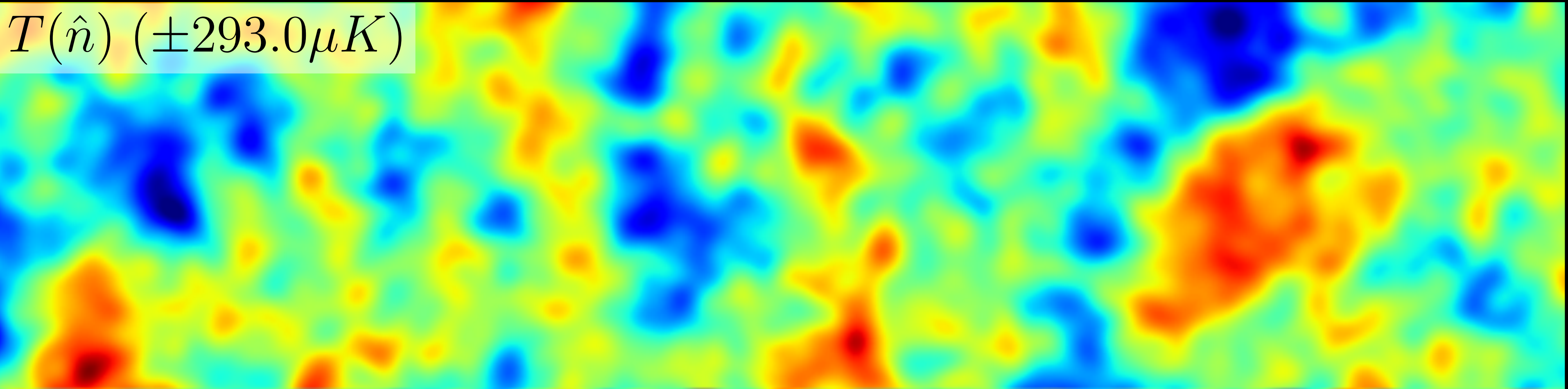


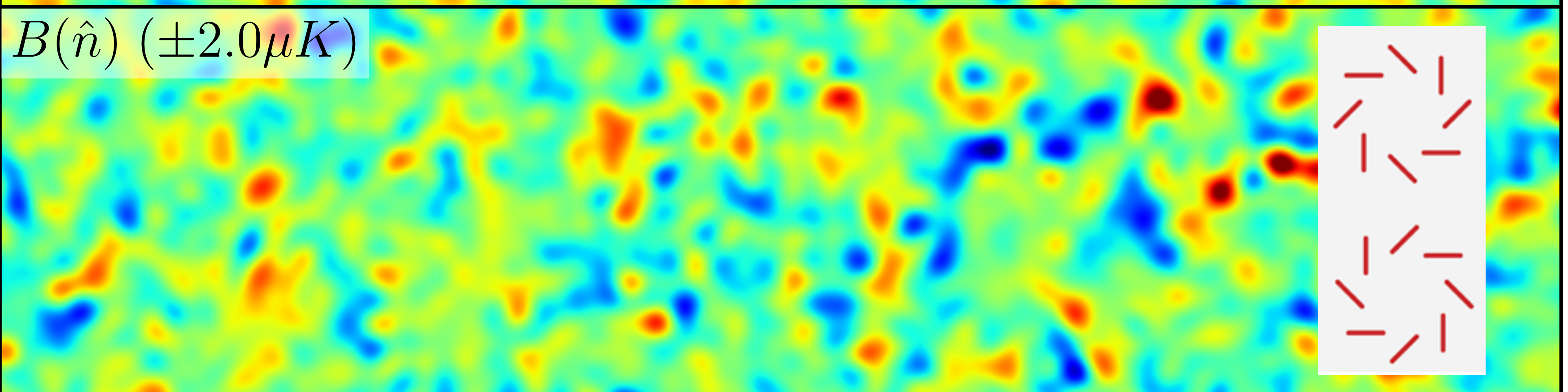
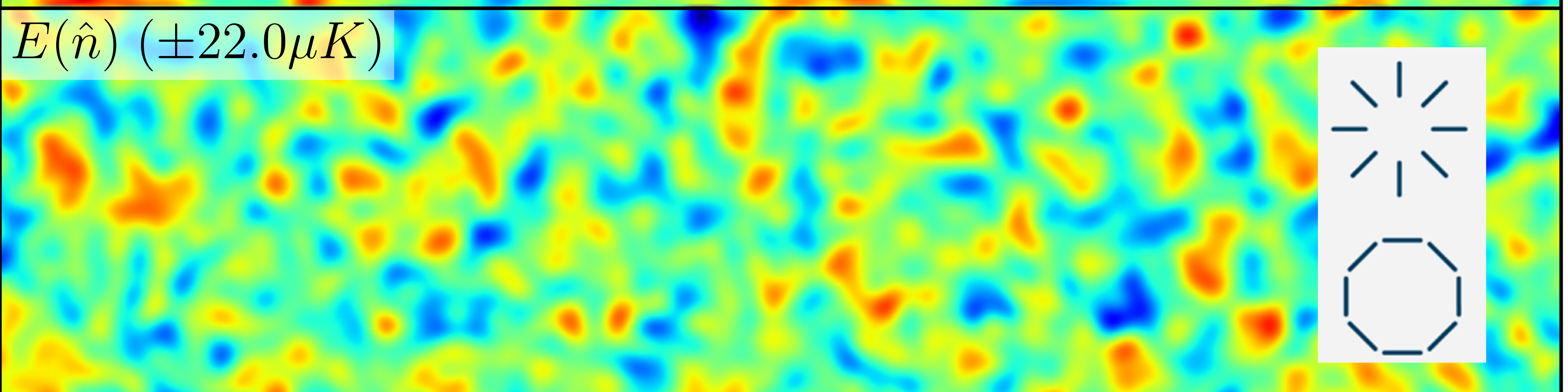
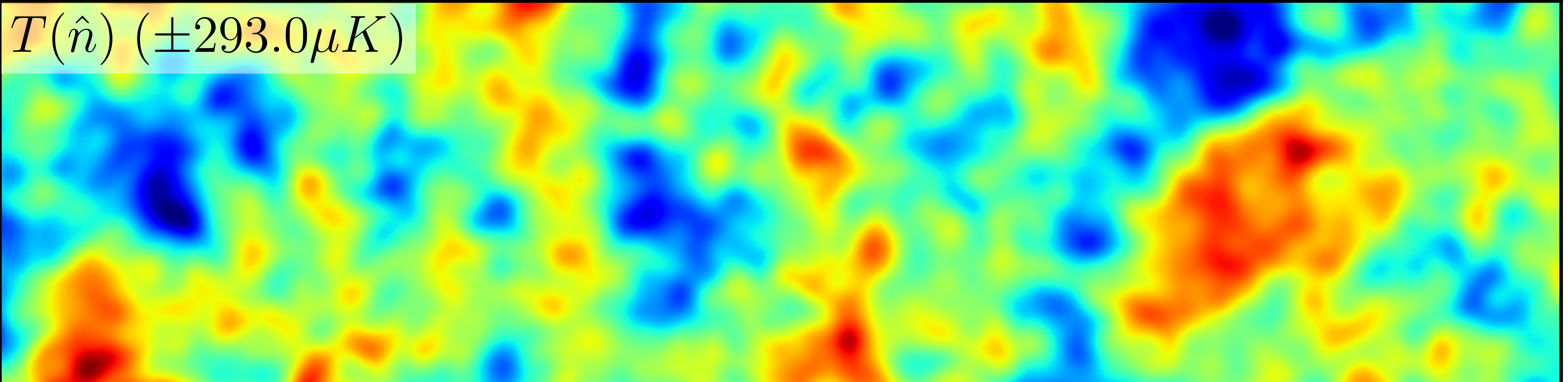
$$\phi(\hat{n}) = -2 \int_0^{\chi_*} d\chi \left(\frac{\chi_* - \chi}{\chi \chi_*} \right) \Psi(\hat{n}, \chi)$$

- Deflections α of a few arcmin by ~ 100 Mpc sized lenses, $\alpha = \nabla \phi$, deflections coherent over a few degrees
- Leading non-linear effect on the CMB
- Most efficient at $z \sim 2$, mostly linear, robust cosmological probe
- Adds and removes information from the CMB

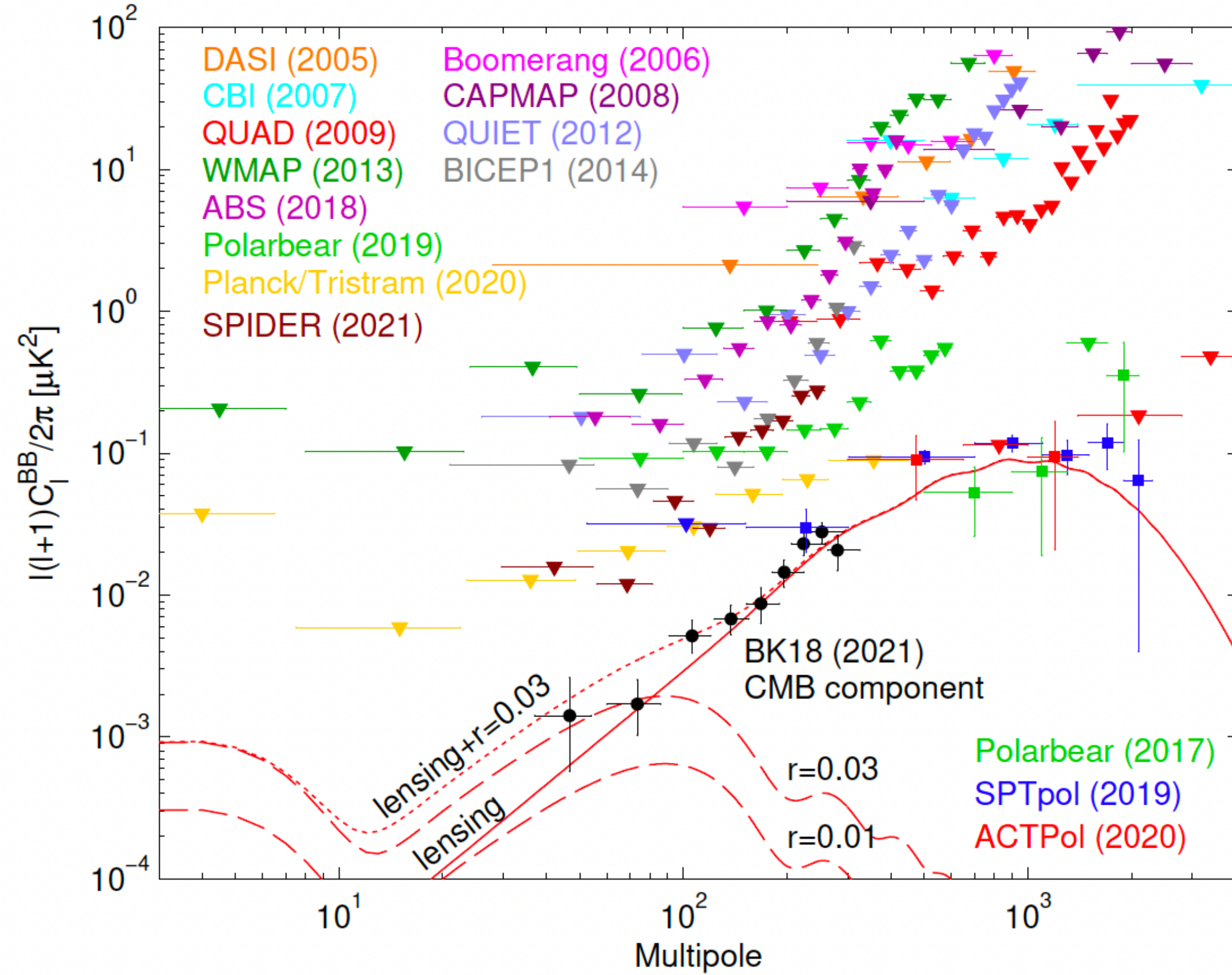
CMB temperature and polarization



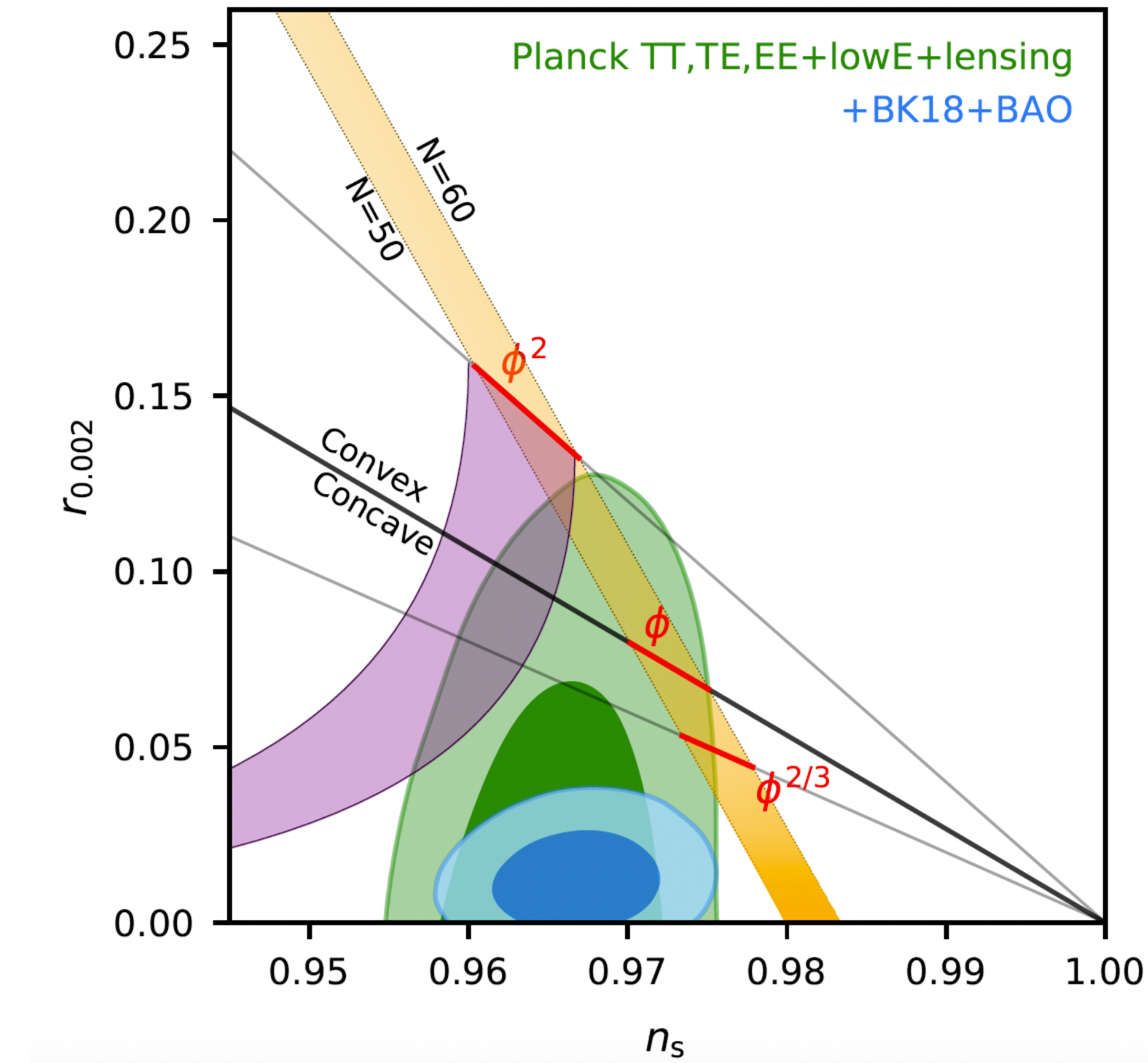




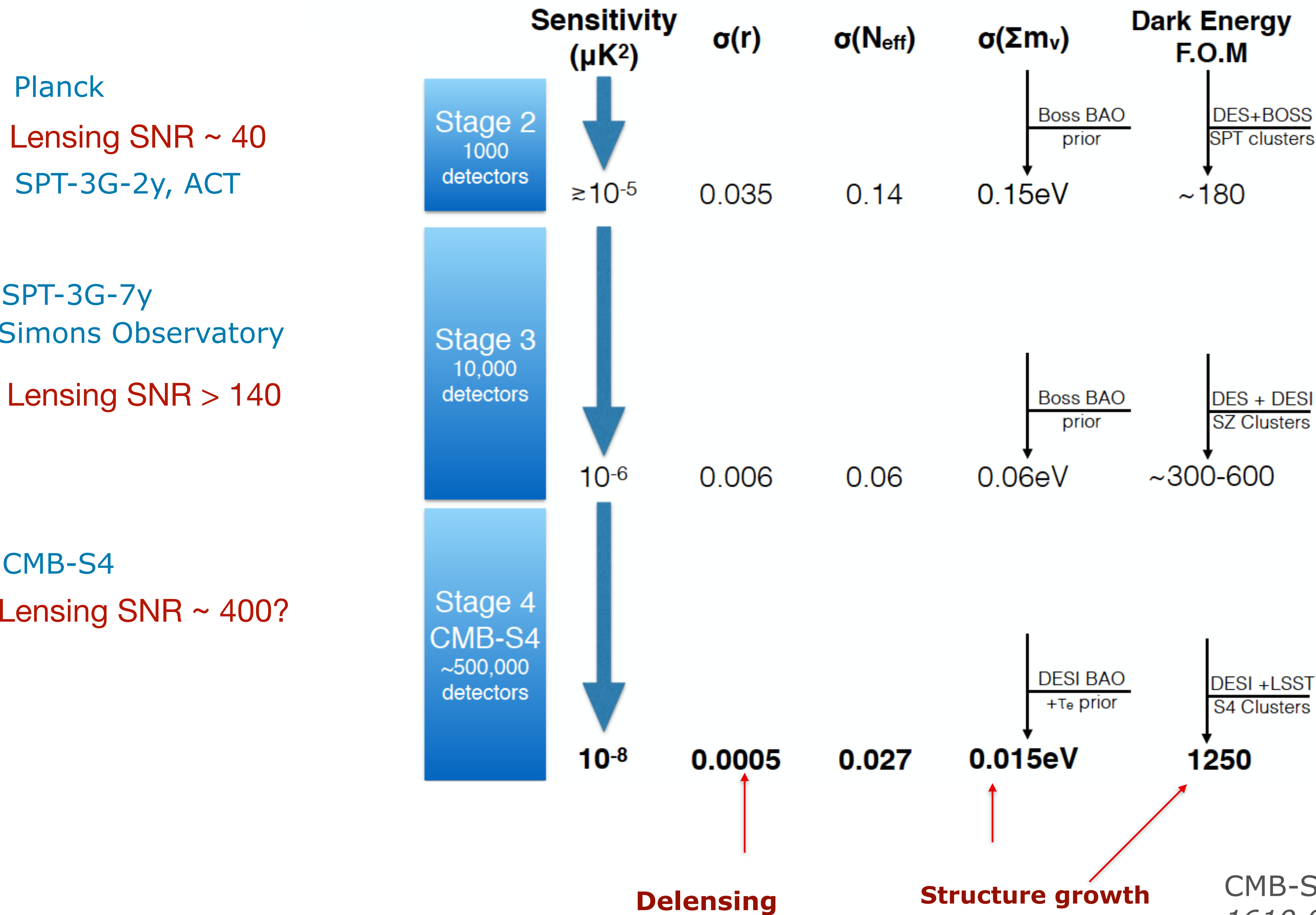
CMB lensing hides information



BICEP / Keck (2021) [2110.00483v1](#)
(and Tristram et al 2021)



$r_{0.05} < 0.032$ (95 % cl)
(limited by lensing now, by a factor of ~ 2)

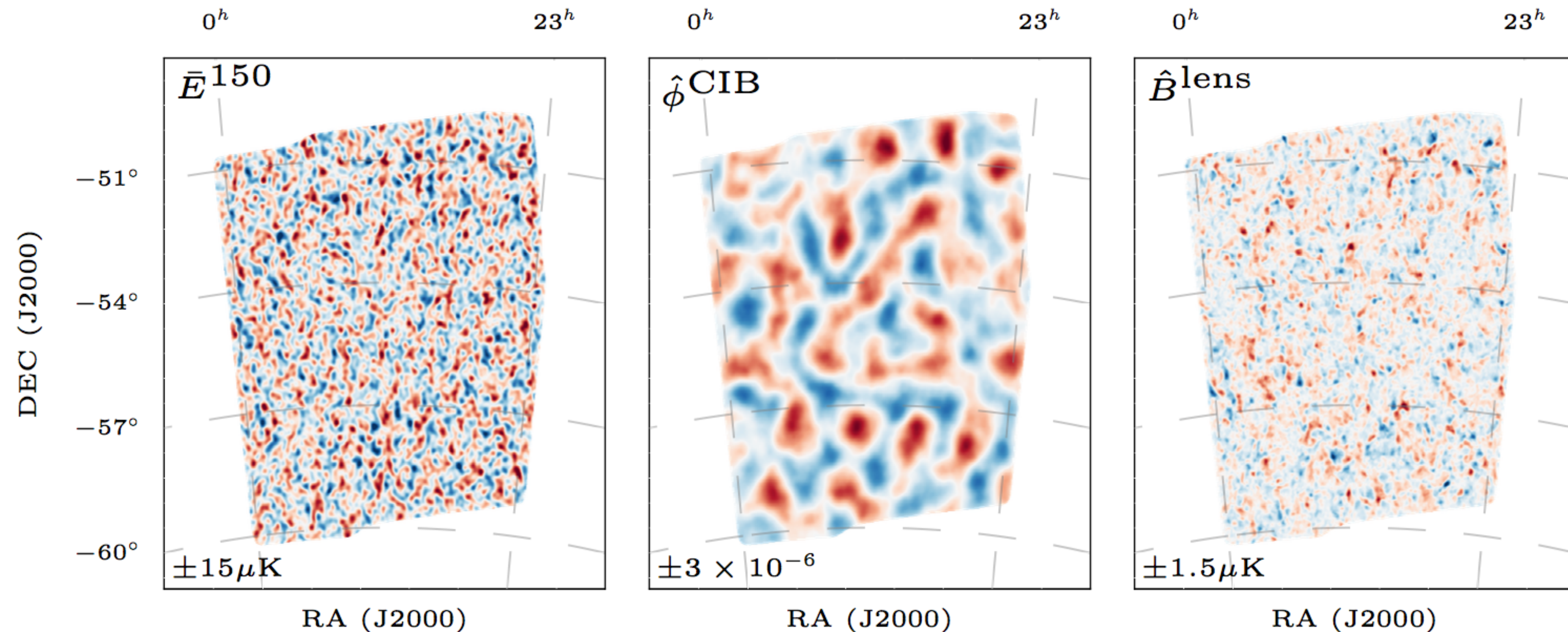


How to delens ?

-Template method :

$$\hat{B}^{\text{lens}}(\boldsymbol{\ell}) = \int \frac{d^2\boldsymbol{\ell}'}{(2\pi)^2} W(\boldsymbol{\ell}, \boldsymbol{\ell}') \bar{E}(\boldsymbol{\ell}') \hat{\phi}(\boldsymbol{\ell} - \boldsymbol{\ell}').$$

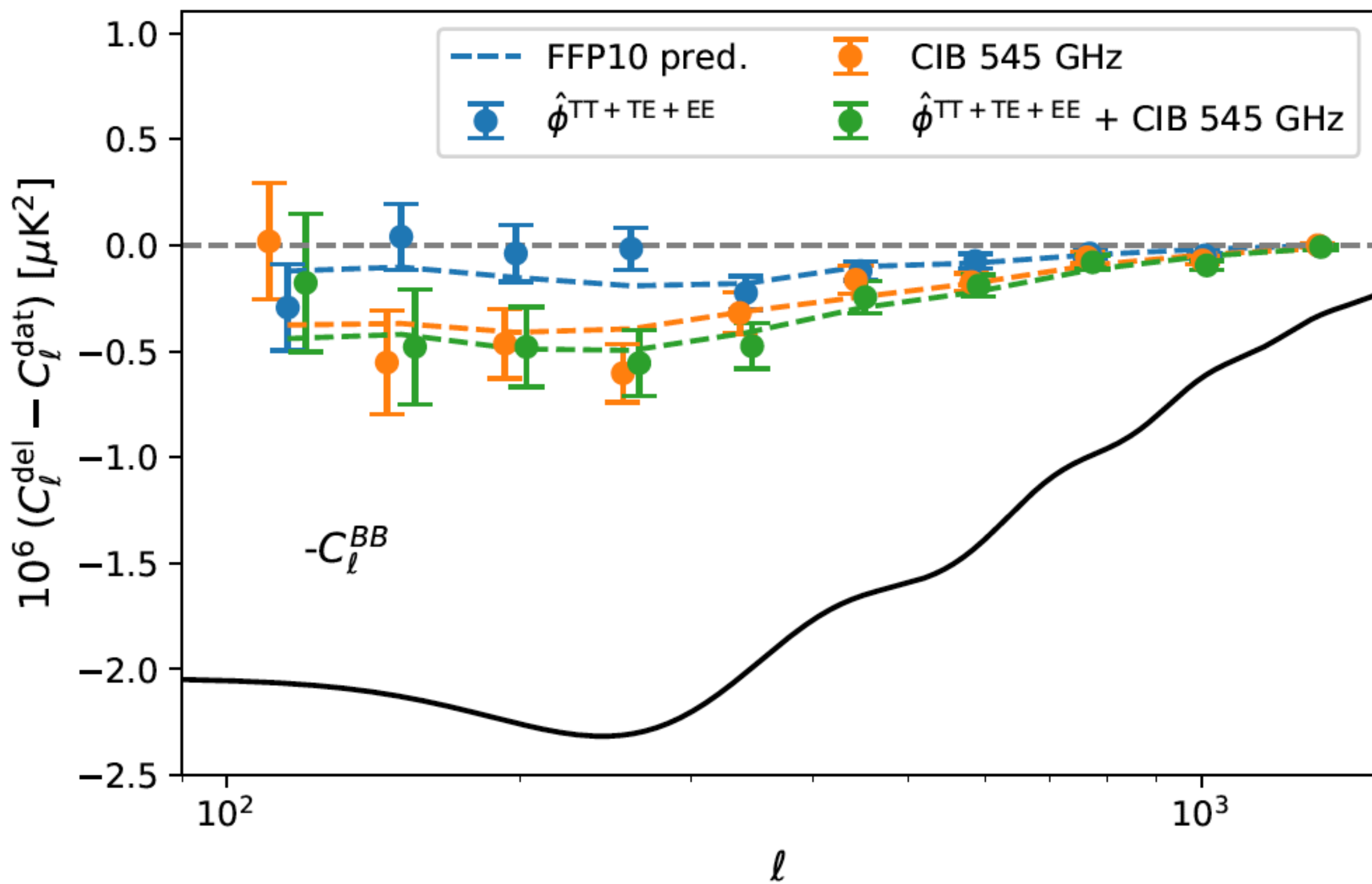
$$B^{\text{del}}(\boldsymbol{\ell}) = B^{\text{meas}}(\boldsymbol{\ell}) - \hat{B}^{\text{lens}}(\boldsymbol{\ell})$$



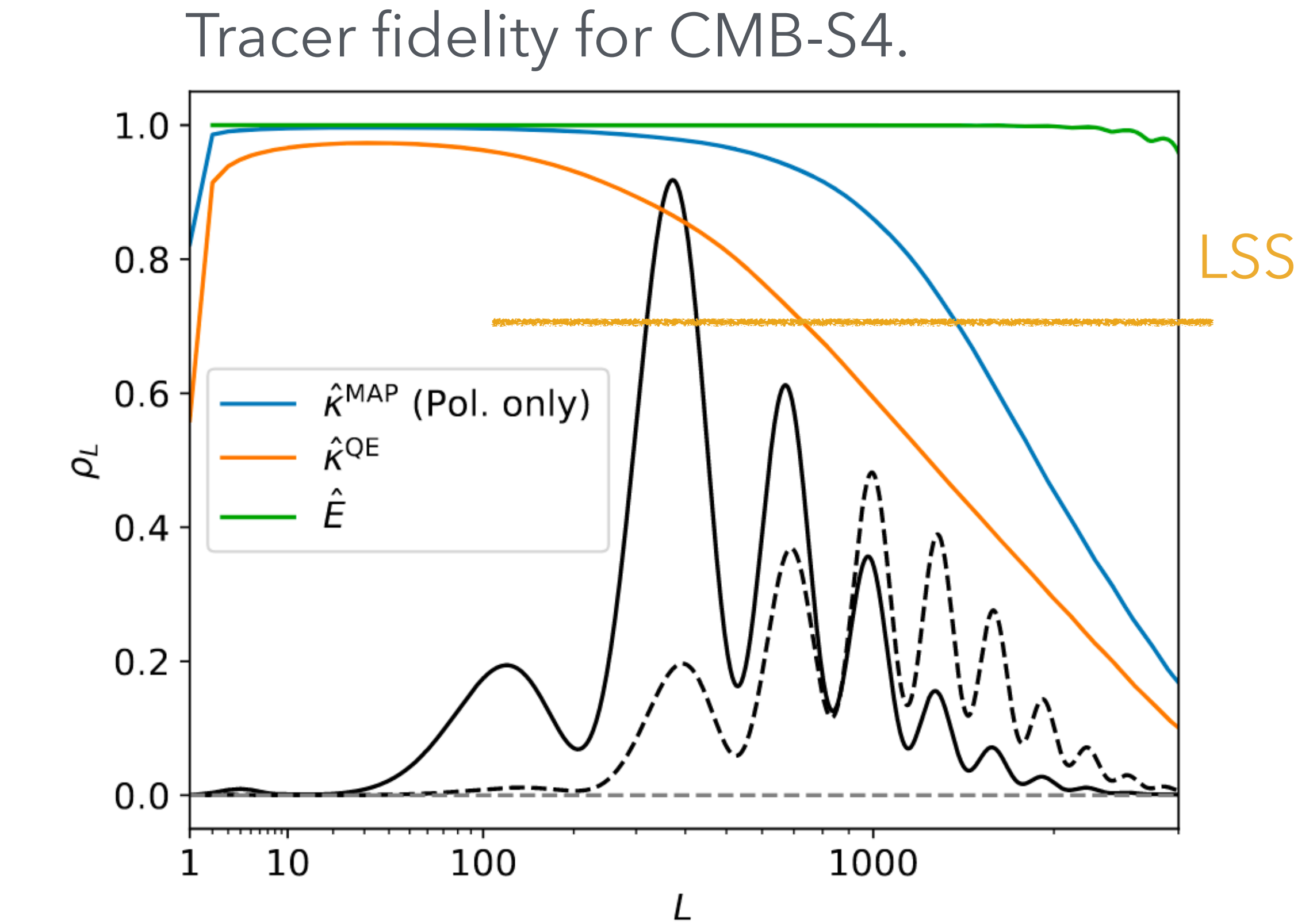
Manzotti et al 1701.04396 (SPT B-mode delensing with CIB)

Also BK-SPTpol 2011.08163

Internal delensing



Here, proof of principle on Planck
data using internal reconstruction
JC, Lewis & Challinor 2017



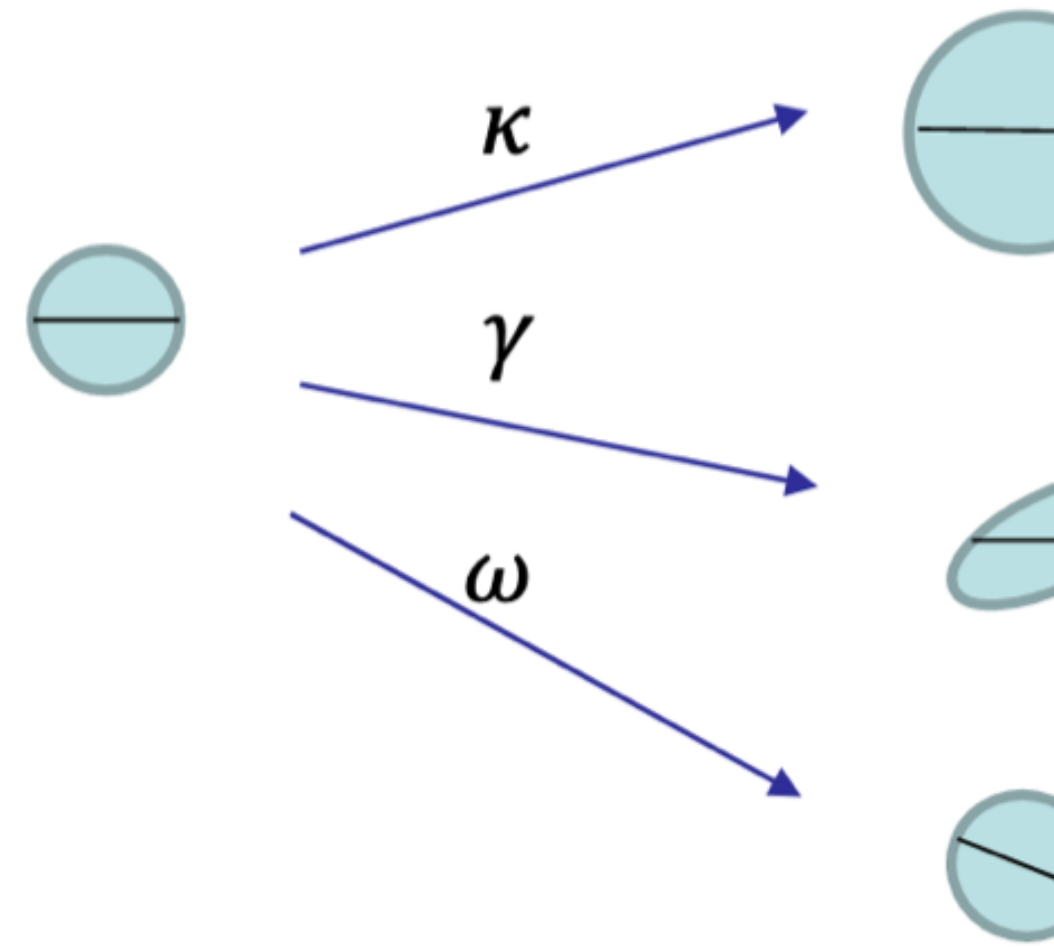
Best delensing will eventually be internal.
Requires exquisite lensing reconstruction
Belkner et al, CMB-S4, 2023

Lensing reconstruction and squeezed limits (high CMB ℓ , low lensing L)

Local effects of large-scale lenses

Deflection related to shear γ_i , convergence κ , and rotation ω

$$A_{ij} \equiv \delta_{ij} + \frac{\partial}{\partial \theta_i} \alpha_j = \begin{pmatrix} 1 - \kappa - \gamma_1 & -\gamma_2 + \omega \\ -\gamma_2 - \omega & 1 - \kappa + \gamma_1 \end{pmatrix}$$



Convergence

Shear

Rotation

$$\kappa = -\frac{1}{2} \nabla \cdot \boldsymbol{\alpha}$$

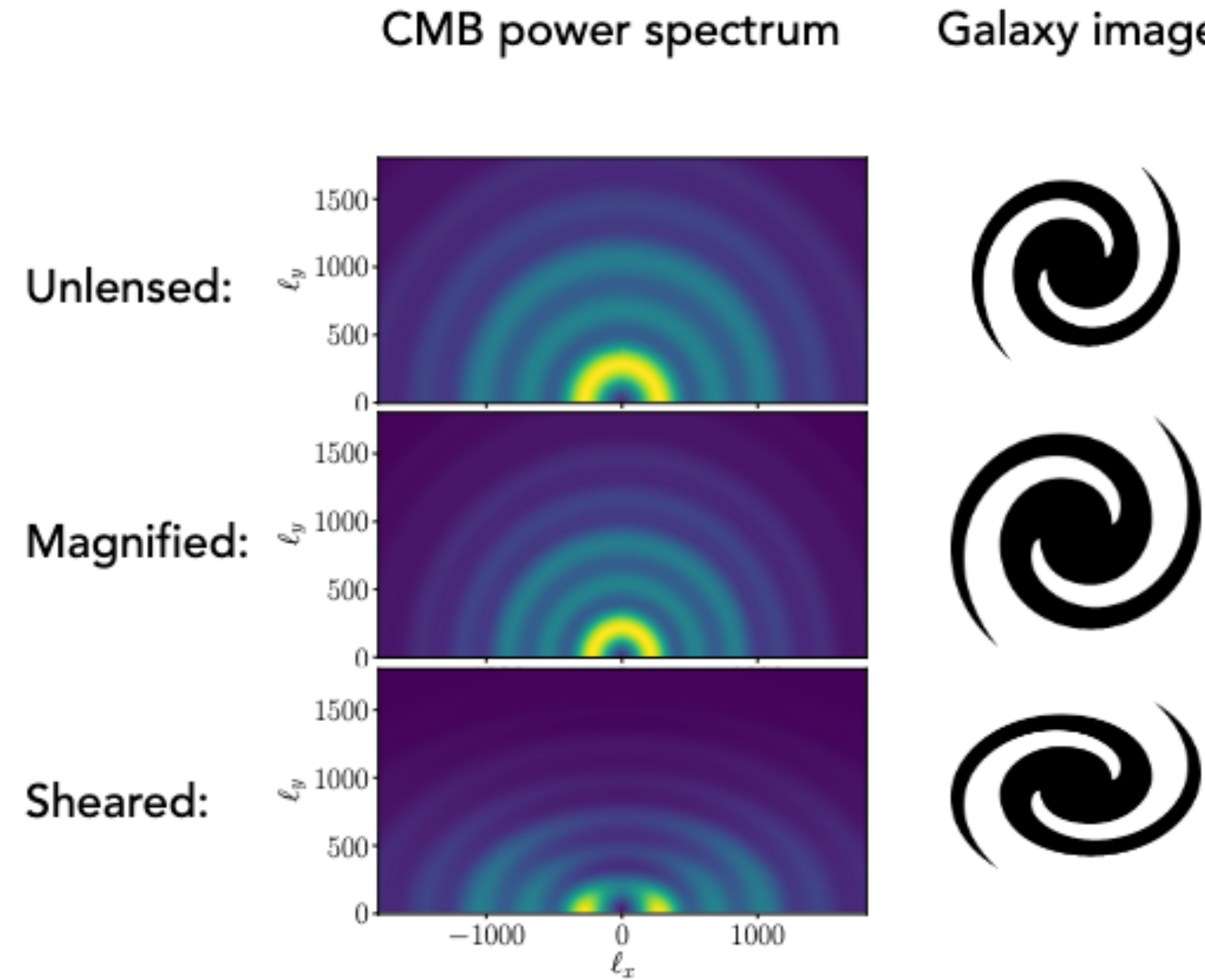
$$\omega(\hat{n}) = -4 \int_0^{\chi_*} d\chi \left(\frac{\chi_* - \chi}{\chi \chi_*} \right) \int_0^\chi d\chi' \left(\frac{\chi - \chi'}{\chi' \chi} \right) \cdot [\gamma_1(\hat{n}, \chi) \gamma_2(\hat{n}, \chi') - \gamma_2(\hat{n}, \chi) \gamma_1(\hat{n}, \chi')]$$

Rotation $\omega = 0$ from scalar perturbations in linear perturbation theory

$$\omega = 0 \Rightarrow \boldsymbol{\alpha} = \nabla \psi$$

Local effects of large-scale lenses

Intensity:



Galaxy image

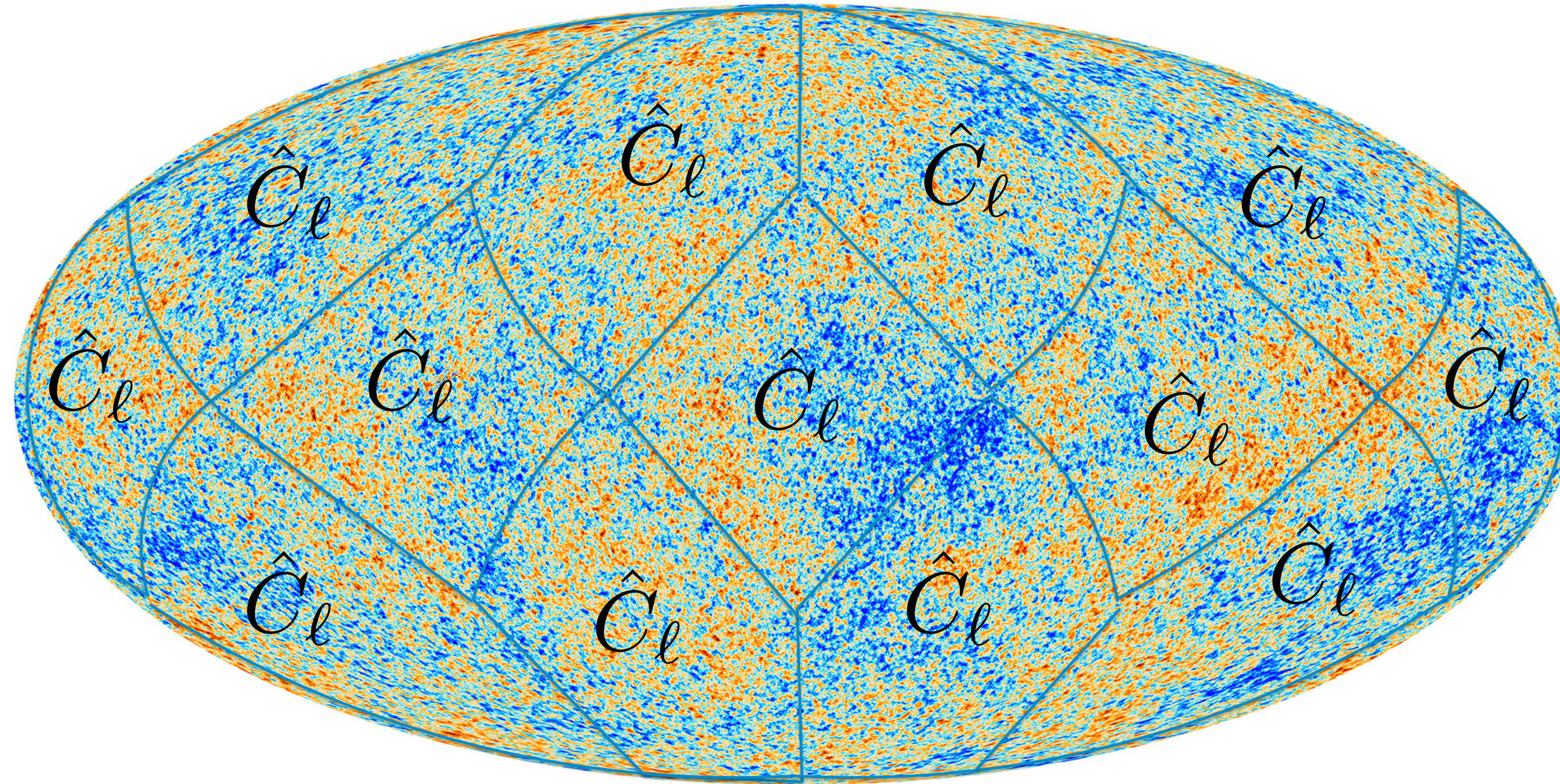
Schaan, Ferraro Spergel 2018



$$\delta C_\ell^{TT} = C_\ell^{TT} \left(1 + \kappa \frac{d \ln \ell^2 C_\ell}{d \ln \ell} + \gamma \cos(2(\phi_\gamma - \phi_\ell)) \frac{d \ln C_\ell}{d \ln \ell} \right)$$

(No impact from local ω here, since rotation locally unobservable)

Quadratic lensing estimation



$$\delta \hat{C}_{\ell}^{TT} = C_{\ell}^{TT} \left(1 + \kappa \frac{d \ln \ell^2 C_{\ell}}{d \ln \ell} + \gamma \cos(2(\phi_{\gamma} - \phi_{\ell})) \frac{d \ln C_{\ell}}{d \ln \ell} \right)$$

Quadratic lensing estimation

- Fixed lenses introduce statistically-anisotropic correlations:

$$\Delta \langle X_{l_1 m_1} Y_{l_2 m_2} \rangle_{\text{CMB}} = \sum_{LM} (-1)^M \begin{pmatrix} l_1 & l_2 & L \\ m_1 & m_2 & -M \end{pmatrix} \mathcal{W}_{l_1 l_2 L}^{XY} \phi_{LM}$$

- Noisy lensing estimates from quadratic CMB combinations:

$$\hat{\phi}_{LM} = \frac{(-1)^M}{2} \frac{1}{\mathcal{R}_L^{XY}} \sum_{l_1 m_1, l_2 m_2} \begin{pmatrix} l_1 & l_2 & L \\ m_1 & m_2 & -M \end{pmatrix} [\mathcal{W}_{l_1 l_2 L}^{XY}]^* \bar{X}_{l_1 m_1} \bar{Y}_{l_2 m_2}$$

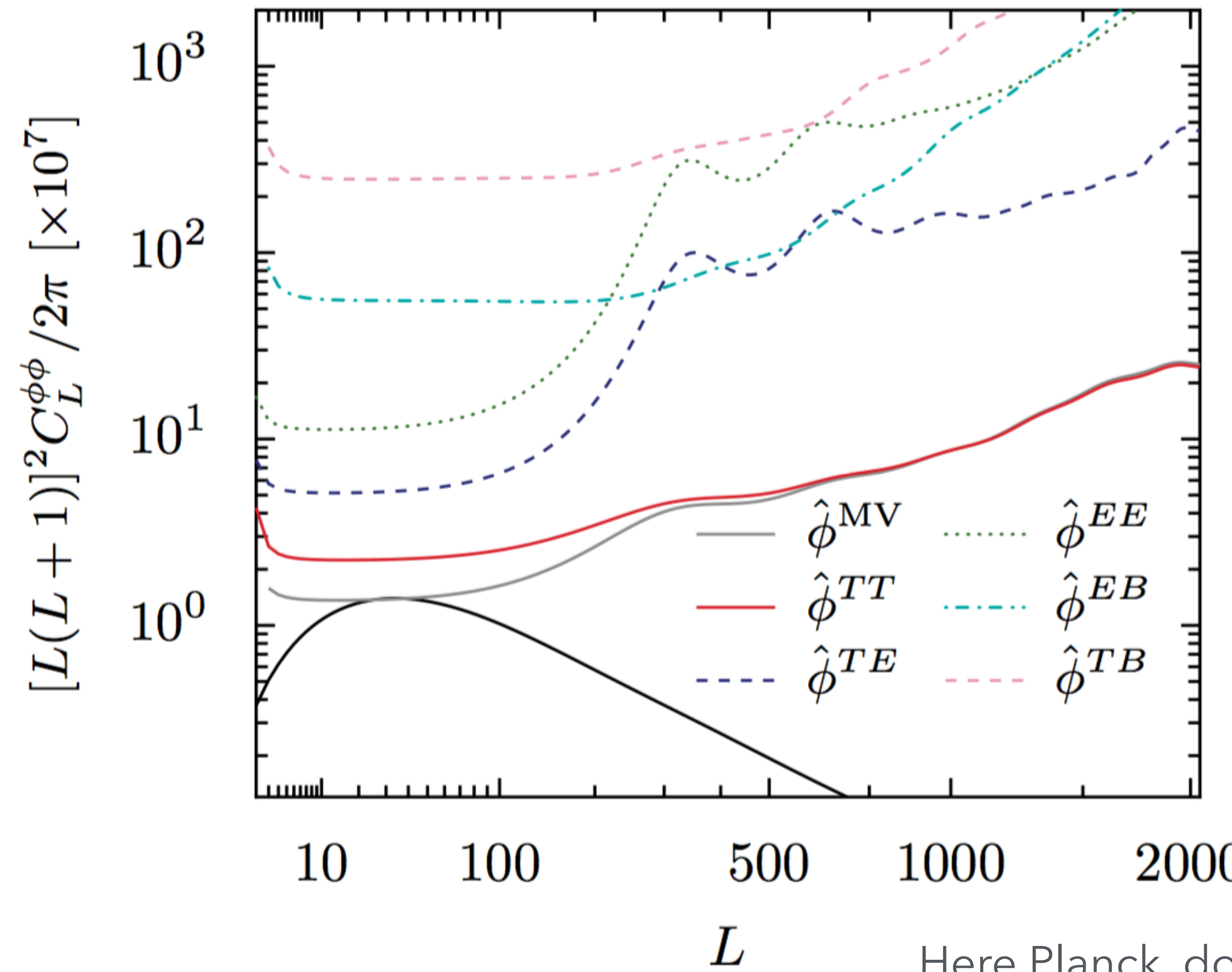
Normalisation

Known lensing-induced correlations

Inverse-variance-weighted CMB fields

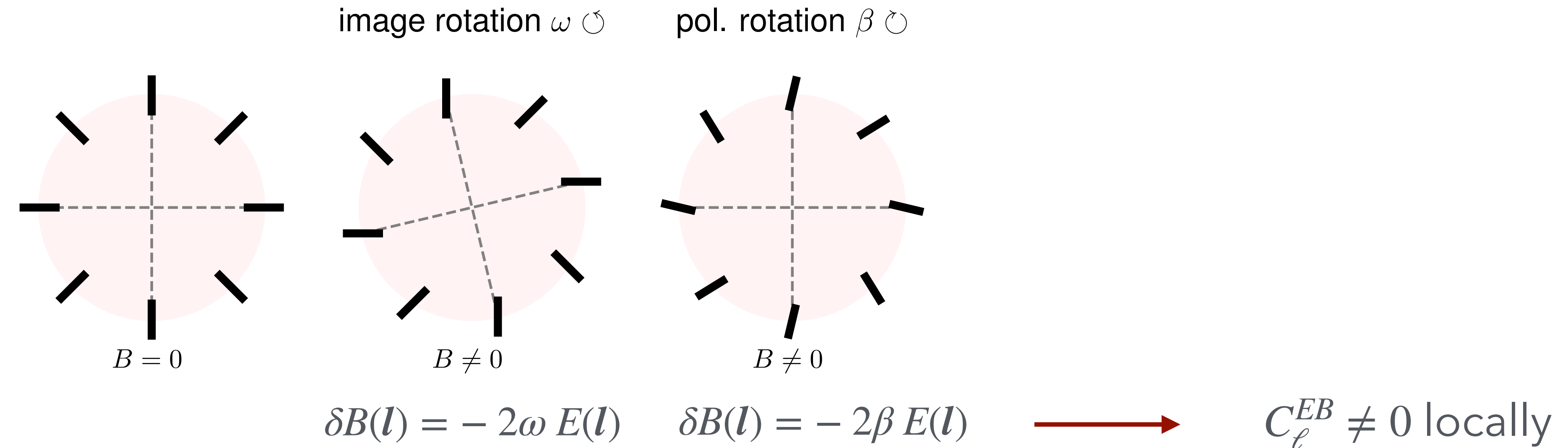
Bispectrum expansions
Schaan & Ferraro 2018 (flat-sky)
JC & Lewis 2024 (curved-sky)

Quadratic estimator reconstruction noise levels:

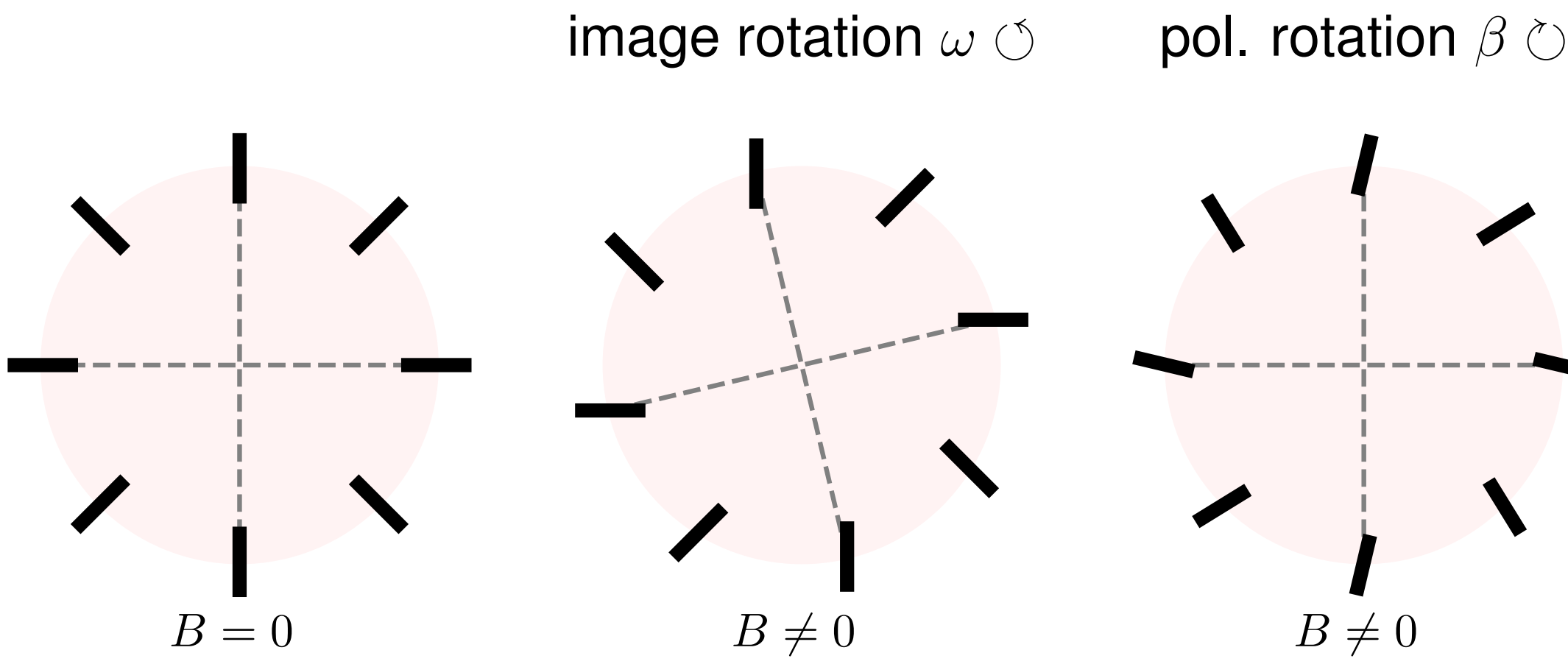


Polarization:

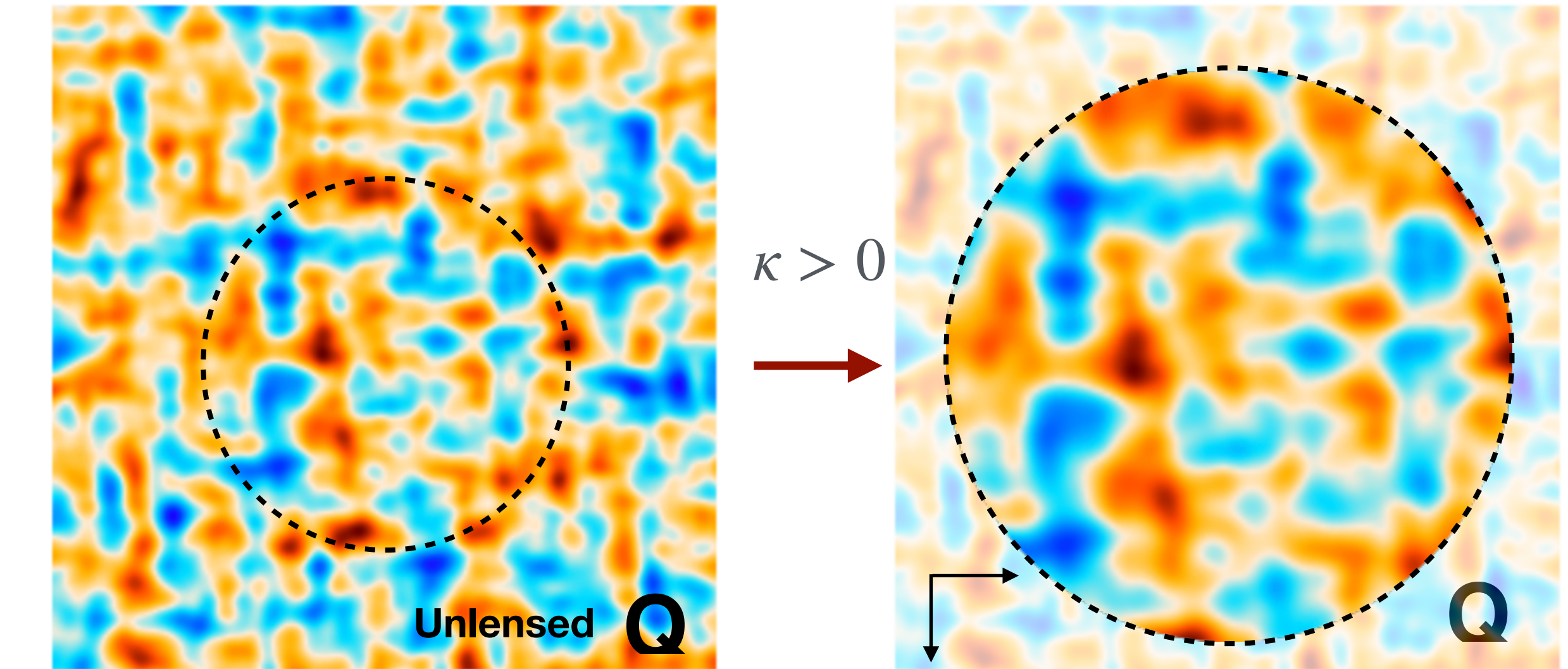
- EE behaves essentially the same as TT
- Since primordial B is small, most relevant is the effect on the local EB spectrum (estimator not limited by primordial fluctuations)



Polarization



$$\delta B(\ell) = -2\omega E(\ell) \quad \delta B(\ell) = -2\beta E(\ell)$$



No impact from local κ on pure E -mode
(standard lensing EB estimator is « shear-only »)

$$\delta C_\ell^{EB} = C_\ell^{EE} \left(\underline{-2\omega} + \underline{-2\beta} + \underline{2\gamma \sin(2(\phi_\gamma - \phi_\ell))} \right)$$

Lensing
rotation

Pol.
rotation

Lensing
local shear, anisotropic squashing

Local reconstruction noise $N_L^{(0)}$

Change in local small-scale EB power spectrum

$$(\text{SNR})^2 \sim \sum_{\ell} \frac{2\ell + 1}{4\pi} \frac{-2C_{\ell}^{EE}}{C_{\ell}^{EE} + N_{\ell}^{EE}} \frac{-2C_{\ell}^{EE}}{C_{\ell}^{BB} + N_{\ell}^{BB}}$$

Number of small scales modes

Lensing power

The diagram illustrates the components of the signal-to-noise ratio squared. It features a central equation: $(\text{SNR})^2 \sim \sum_{\ell} \frac{2\ell + 1}{4\pi} \frac{-2C_{\ell}^{EE}}{C_{\ell}^{EE} + N_{\ell}^{EE}} \frac{-2C_{\ell}^{EE}}{C_{\ell}^{BB} + N_{\ell}^{BB}}$. Three red arrows point to specific parts of the equation: one arrow points from the factor $\frac{2\ell + 1}{4\pi}$ to the text "Number of small scales modes"; another arrow points from the two terms $-2C_{\ell}^{EE}$ to the text "Lensing power"; and a third arrow points from the text "Change in local small-scale EB power spectrum" to the entire equation.

Local reconstruction noise $N_L^{(0)}$

Change in local small-scale EB power spectrum

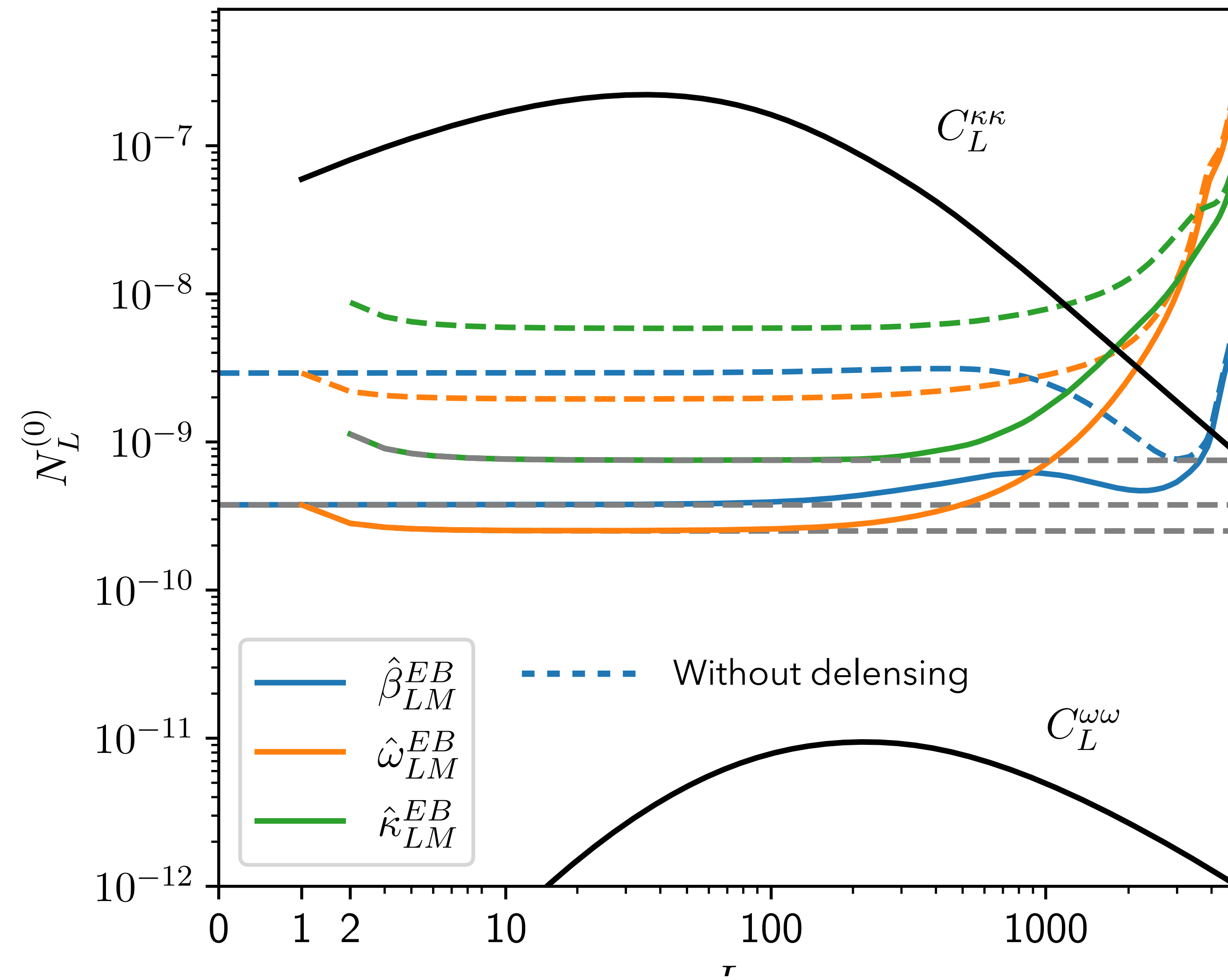
$$(\text{SNR})^2 \sim \sum_{\ell} \frac{2\ell + 1}{4\pi} \frac{-2C_{\ell}^{EE}}{C_{\ell}^{EE} + N_{\ell}^{EE}} \frac{-2C_{\ell}^{EE}}{C_{\ell}^{BB} + N_{\ell}^{BB}} \times \begin{cases} 1 & (\text{polarization rotation } \beta) \\ \sim 3/2 & (\text{curl lensing } \omega) \\ \sim 1/2 & (\text{gradient lensing } \kappa) \end{cases}$$

Number of small scales modes

Lensing power

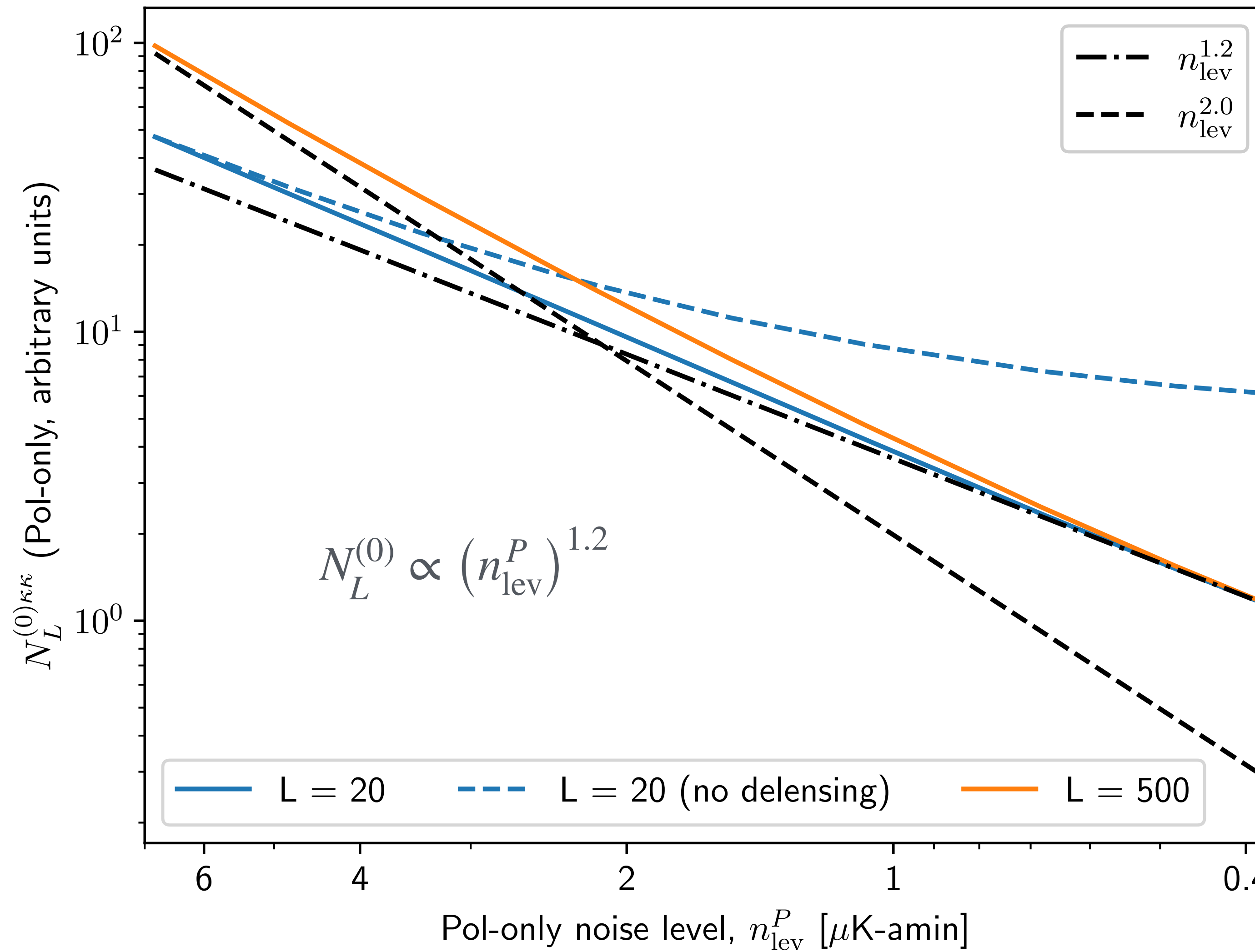
Change in local small-scale EB power spectrum

CMB-S4 deep alike

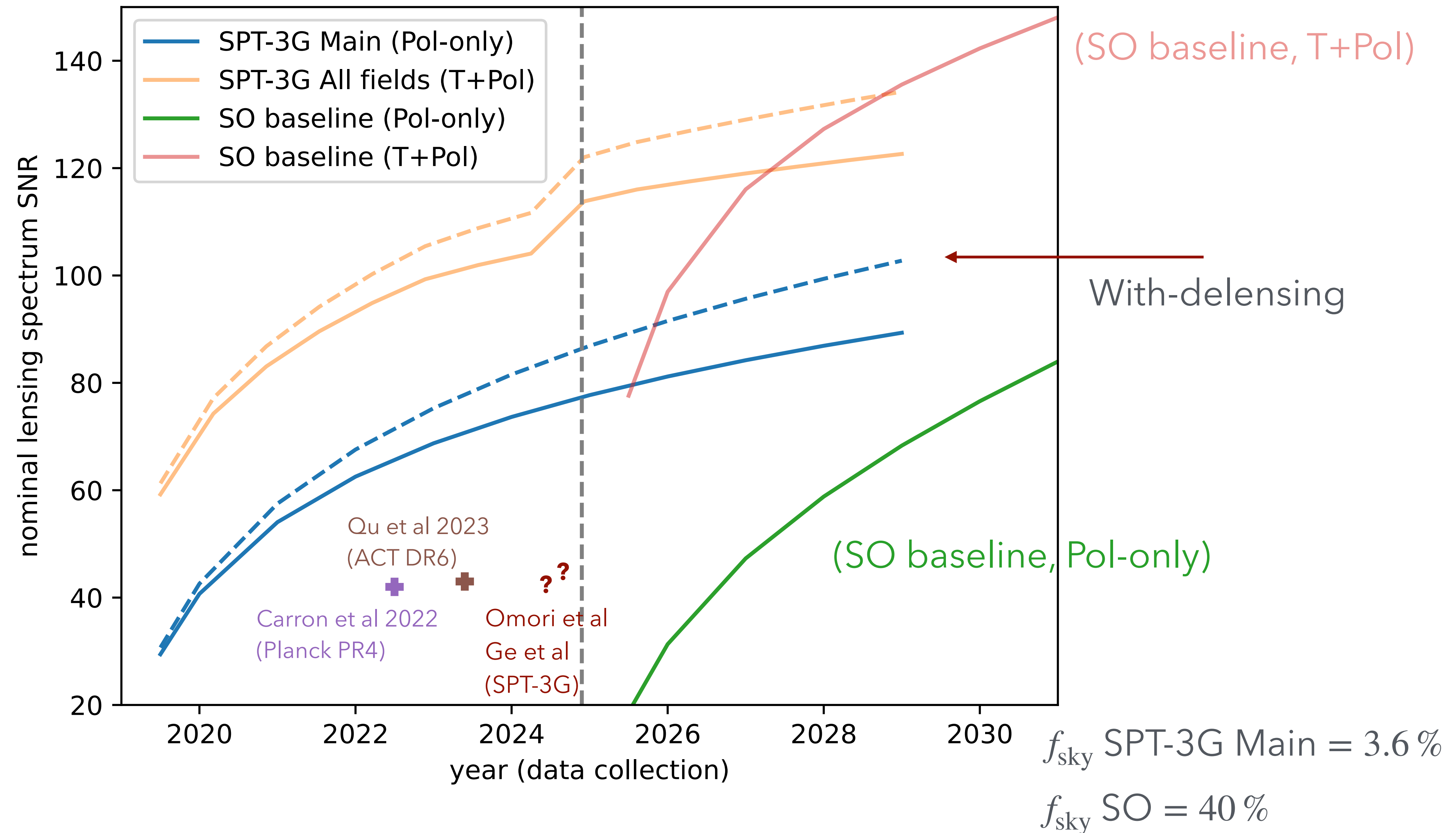


κ : lensing gradient (standard) mode
 β : polarization rotation
 ω : lensing curl mode

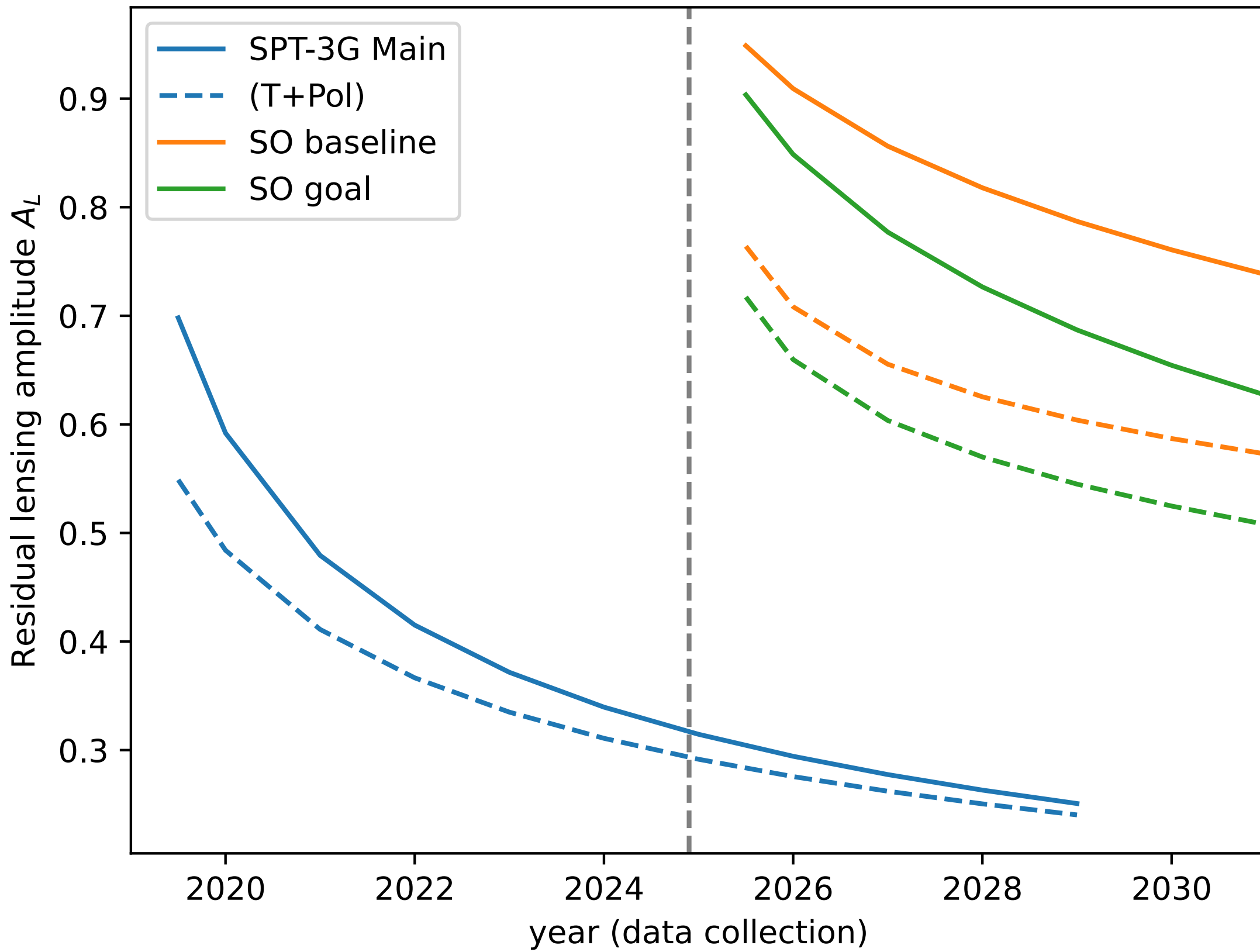
Deeper vs wider



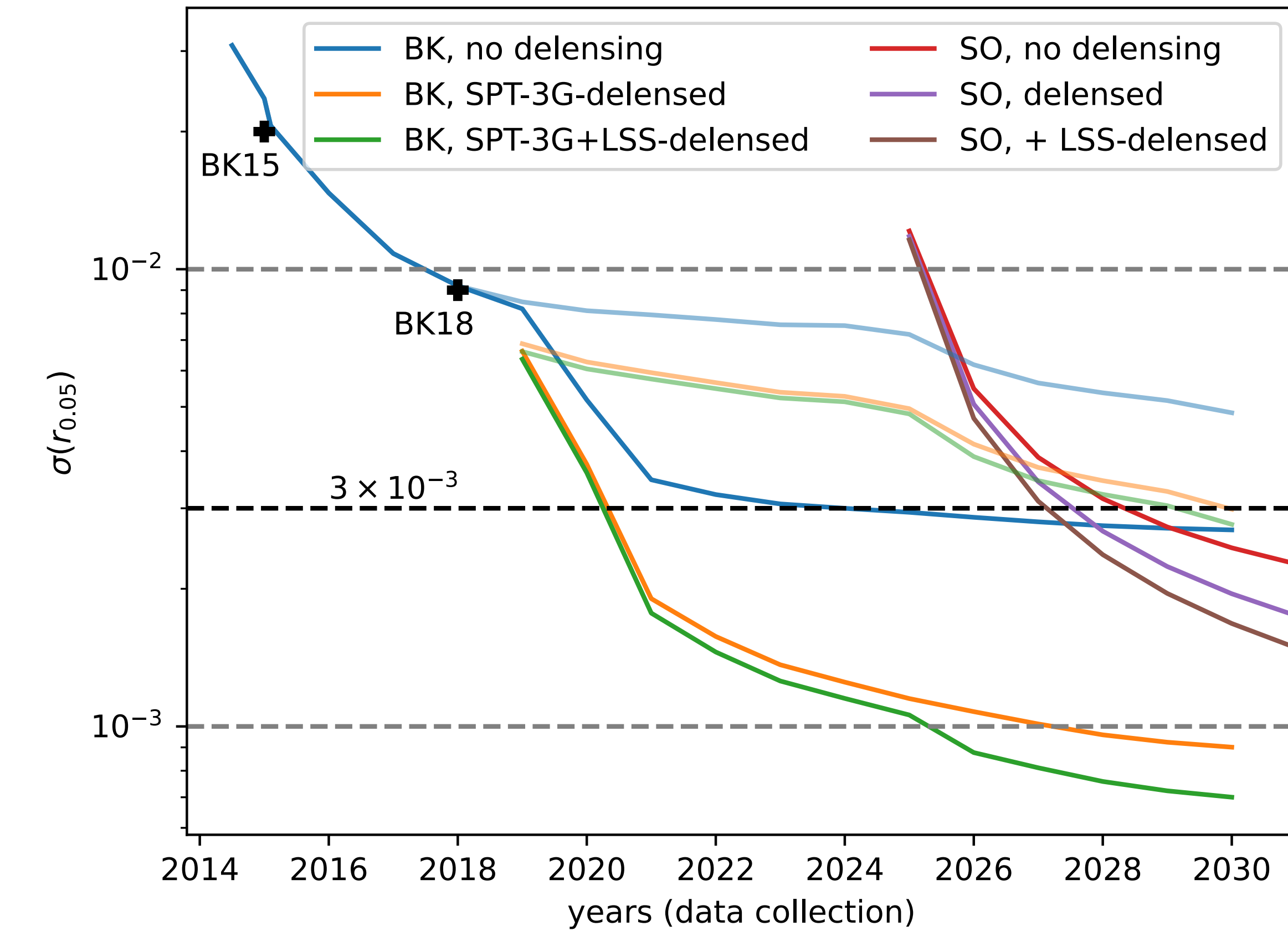
Lensing spectrum SNR in the near future (NB: cosmic variance limited on a wide range of scales!)



Delensing capabilities in the near future

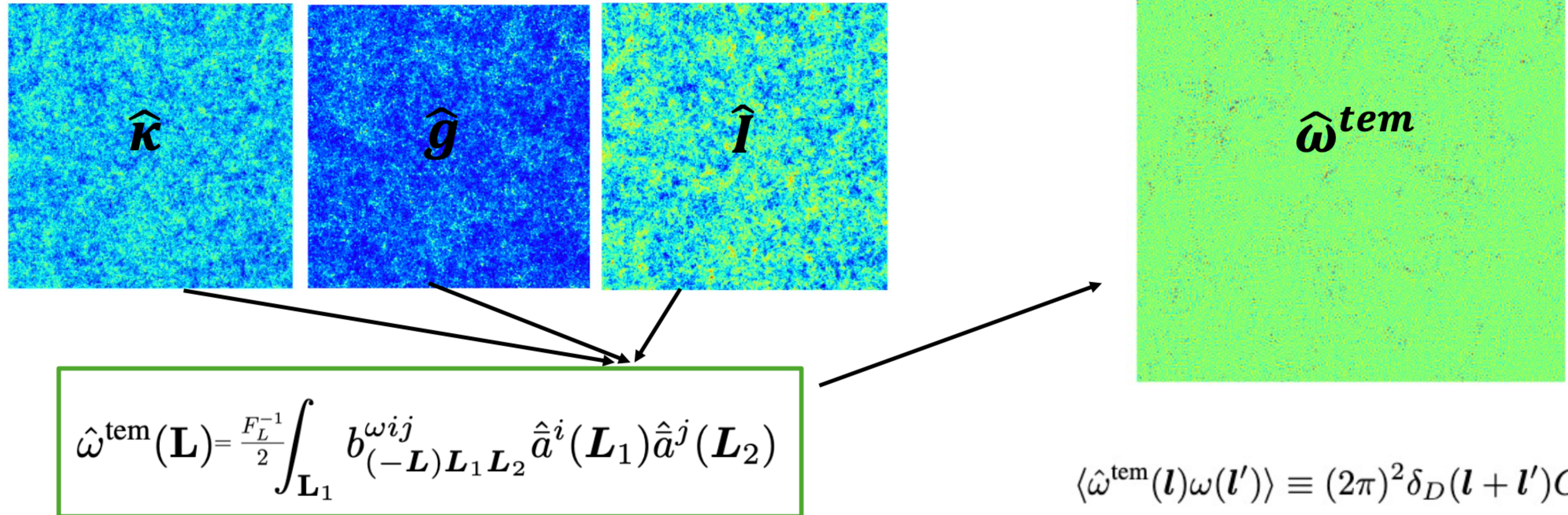


Achievable residual lensing amplitude



Constraints on r

Lensing curl detection in x-correlation to LSS



Slide M.Robertson

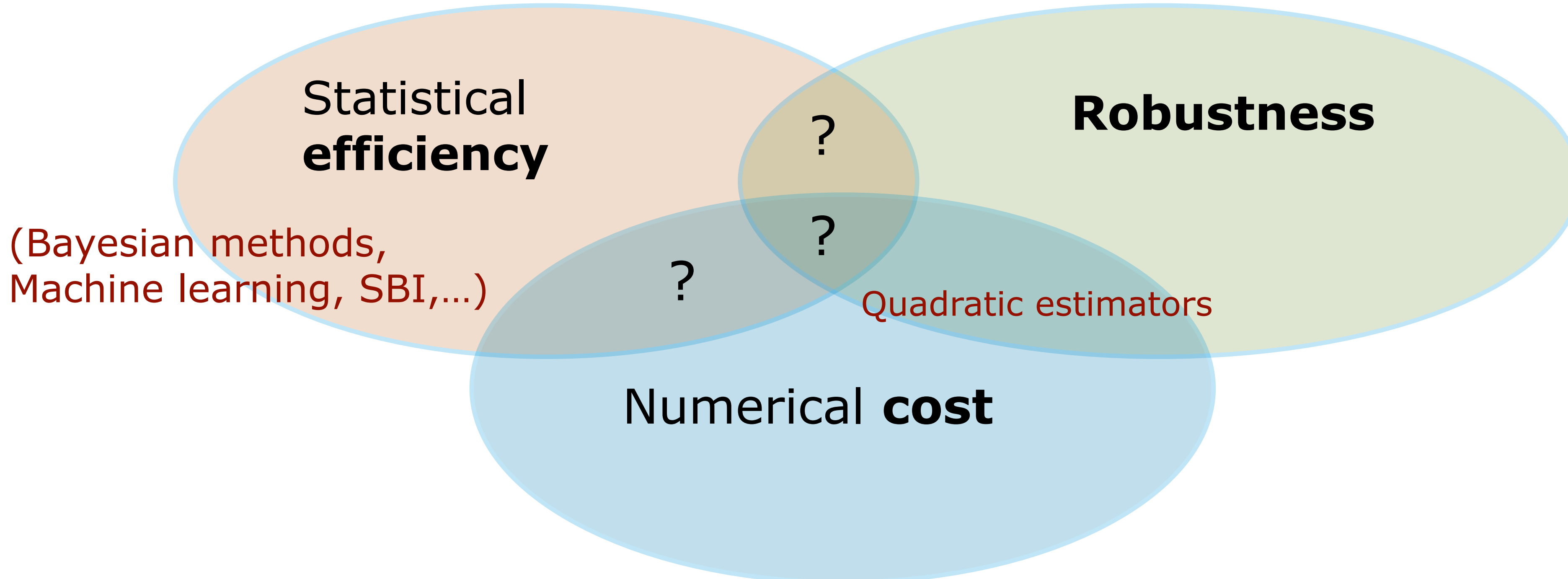
Want to detect $\langle \hat{\omega} \hat{\omega}^{\text{tem}} \rangle$

Lensing curl-mode detection (in combination with LSS)

	$100 \cdot f_{\text{sky}}$	$\omega[\kappa, g]$	$\omega[\kappa, I]$	$\omega[g, I]$	$\omega[\kappa, g, I]$	
LiteBird ($L_{\text{max}} = 1200$)	60	0.7	0.1	0.9	1.1	
SO-baseline	40	1.8	0.4	2.5	2.9	
SO-baseline (GMV)	40	3.4	0.6	3.7	4.6	$f_{\text{sky}} = 40\%$
SO-goal	40	3.3	0.6	3.6	4.5	
SO-goal (GMV)	40	4.7	0.8	4.6	6.0	
SPT-3G (2019-2026)	3.6	4.5	0.8	3.2	4.9	$f_{\text{sky}} = 3.6\%$
PICO	60	29.5	5.6	18.6	31.2	
S4-wide	40	22.4	4.1	14.8	23.9	
S4-deep	3.6	24.0	4.2	13.3	24.9	

« Bayesian » lensing reconstruction

Serious challenges facing « optimal lensing » methods...

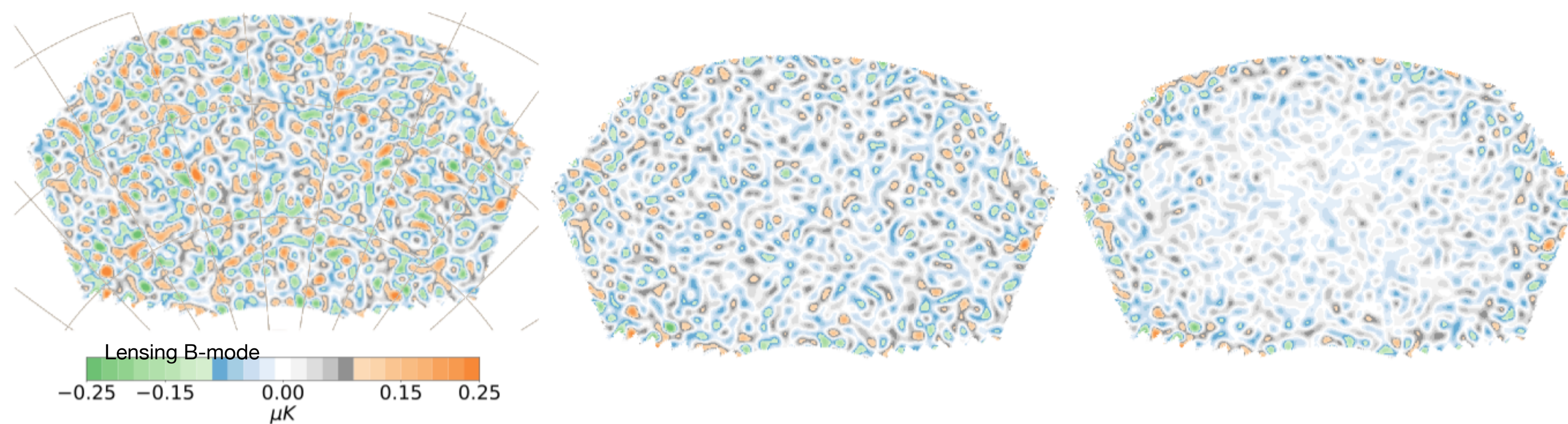
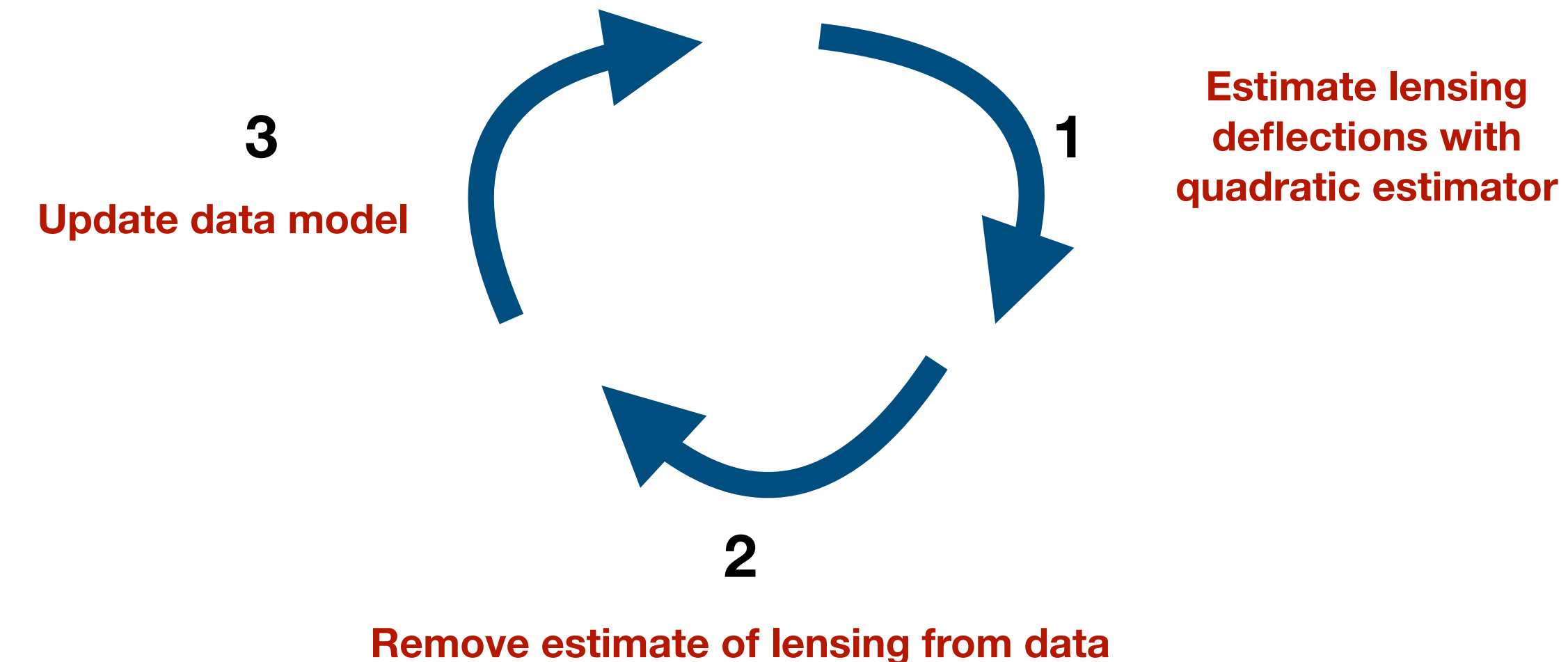


1. A precise characterization of the output is much more difficult, in fact often just intractable, even under idealized experimental configurations.
2. The reliance on the accuracy of every parts of the likelihood model. Full understanding of some parts of the data is never possible. It is difficult to anticipate how this will affect a Bayesian-like lensing method.
3. An heavier computational load, sometimes by absolutely massive amounts.

MAP (Maximum A Posteriori reconstruction)

Hirata & Seljak 2003, JC & Lewis 2017, Legrand & JC 2022, 2023

Arguably the simplest yet efficient method



CMB lensing likelihood.

$$-\ln p(X^{\text{dat}} | \phi) = \frac{1}{2} X^{\text{dat}} \underline{\text{Cov}}_{\phi}^{-1} X^{\text{dat}} + \frac{1}{2} \ln \det \text{Cov}_{\phi}$$

Anisotropic CMB spectra

(Hirata & Seljak 2003, JC & Lewis 2017)

CMB lensing likelihood.

$$-\ln p(X^{\text{dat}} | \phi) = \frac{1}{2} X^{\text{dat}} \underline{\text{Cov}}_{\phi}^{-1} X^{\text{dat}} + \frac{1}{2} \ln \det \text{Cov}_{\phi}$$

Anisotropic CMB spectra

(Hirata & Seljak 2003, JC & Lewis 2017)

Typical likelihood model is a **compromise between fidelity and numerical cost**:

$$\text{Cov}_{\phi} = T D_{\phi} C^{EE} D_{\phi}^{\dagger} T^{\dagger} + N$$

Beam, transfer function

Lensing

Unlensed E spectrum

Noise covariance matrix

```
graph LR; T[TD_phi] --> CEE[C^{EE}]; D[D_phi_dagger] --> CEE; N[N] --> CEE; subgraph Labels; direction LR; Beam[Beam, transfer function] --> TD_phi; Lensing[Lensing] --> CEE; Unlensed[Unlensed E spectrum] --> D_phi_dagger; Noise[Noise covariance matrix] --> N; end;
```

CMB lensing likelihood.

$$-\ln p(X^{\text{dat}} | \phi) = \frac{1}{2} X^{\text{dat}} \underline{\text{Cov}}_{\phi}^{-1} X^{\text{dat}} + \frac{1}{2} \ln \det \text{Cov}_{\phi}$$

Anisotropic CMB spectra

(Hirata & Seljak 2003, JC & Lewis 2017)

Likelihood gradients w.r.t. to ϕ_{LM} :

$$g_{\phi} = g_{\phi}^{\text{QD}} - \left\langle g_{\phi}^{\text{QD}} \right\rangle$$



CMB lensing likelihood.

$$-\ln p(X^{\text{dat}} | \phi) = \frac{1}{2} X^{\text{dat}} \underline{\text{Cov}}_{\phi}^{-1} X^{\text{dat}} + \frac{1}{2} \ln \det \text{Cov}_{\phi}$$

Anisotropic CMB spectra

(Hirata & Seljak 2003, JC & Lewis 2017)

Likelihood gradients w.r.t. to ϕ_{LM} :

$$g_{\phi} = g_{\phi}^{\text{QD}} - \left\langle g_{\phi}^{\text{QD}} \right\rangle$$

An ordinary optimized QE, but
acting on maps delensed by
 $\nabla \phi$

CMB lensing likelihood.

$$-\ln p(X^{\text{dat}} | \phi) = \frac{1}{2} X^{\text{dat}} \underline{\text{Cov}}_{\phi}^{-1} X^{\text{dat}} + \frac{1}{2} \ln \det \text{Cov}_{\phi}$$

Anisotropic CMB spectra

(Hirata & Seljak 2003, JC & Lewis 2017)

Likelihood gradients w.r.t. to ϕ_{LM} :

$$g_{\phi} = g_{\phi}^{\text{QD}} - \left\langle g_{\phi}^{\text{QD}} \right\rangle$$

An ordinary optimized QE, but
acting on maps delensed by
 $\nabla \phi$

«Mean-field ». Its
dependence on ϕ is the
only truly novel aspect
compared to QE

CMB lensing likelihood.

$$-\ln p(X^{\text{dat}} | \phi) = \frac{1}{2} X^{\text{dat}} \underline{\text{Cov}}_{\phi}^{-1} X^{\text{dat}} + \frac{1}{2} \ln \det \text{Cov}_{\phi}$$

Anisotropic CMB spectra

(Hirata & Seljak 2003, JC & Lewis 2017)

Likelihood gradients w.r.t. to ϕ_{LM} :

$$g_{\phi} = g_{\phi}^{\text{QD}} - \langle g_{\phi}^{\text{QD}} \rangle$$

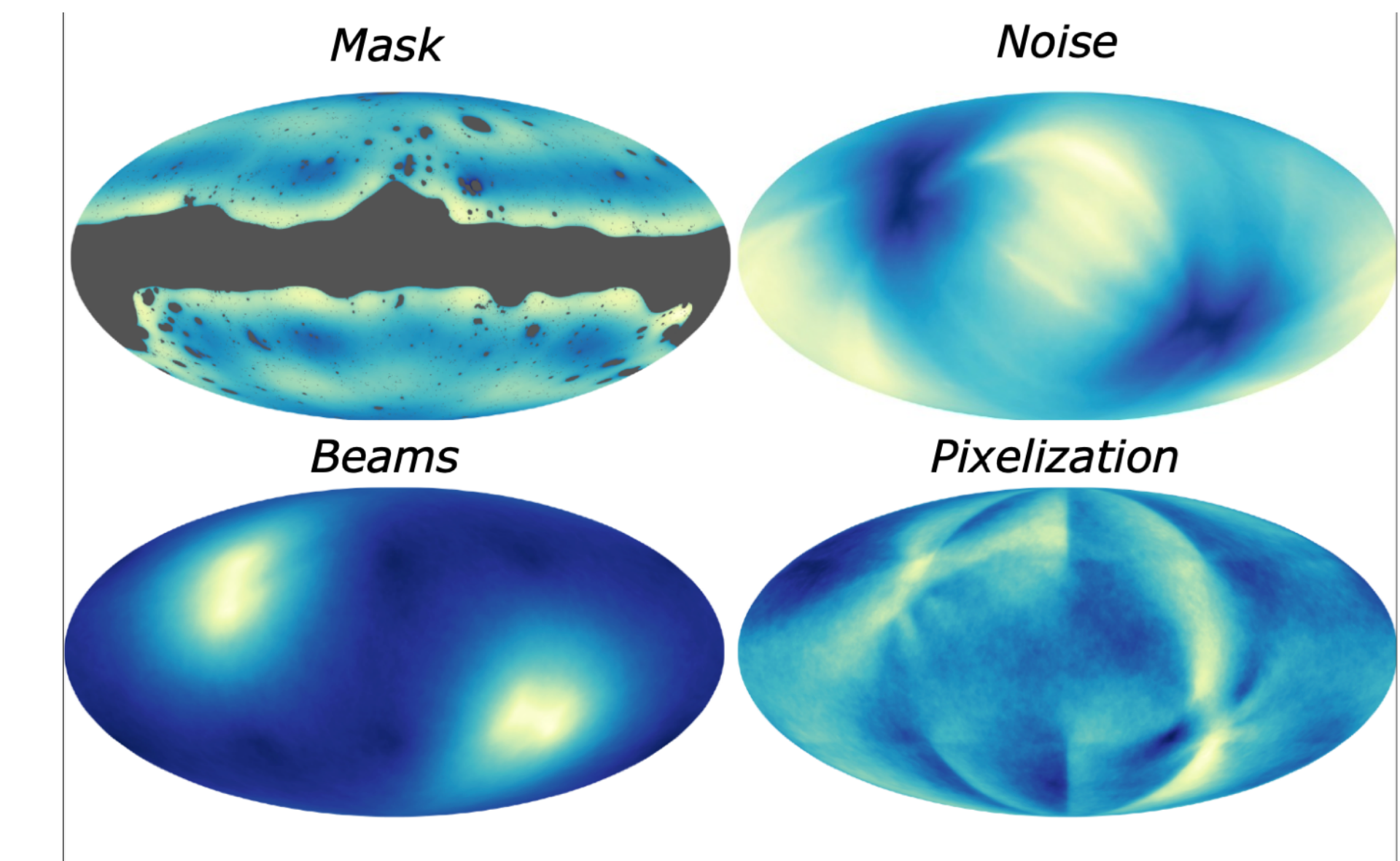
An ordinary optimized QE, but
acting on maps \hat{X}^{WF} delensed
by $\nabla \phi$

«Mean-field ». Its
dependence on ϕ is the
only truly novel aspect
compared to QE

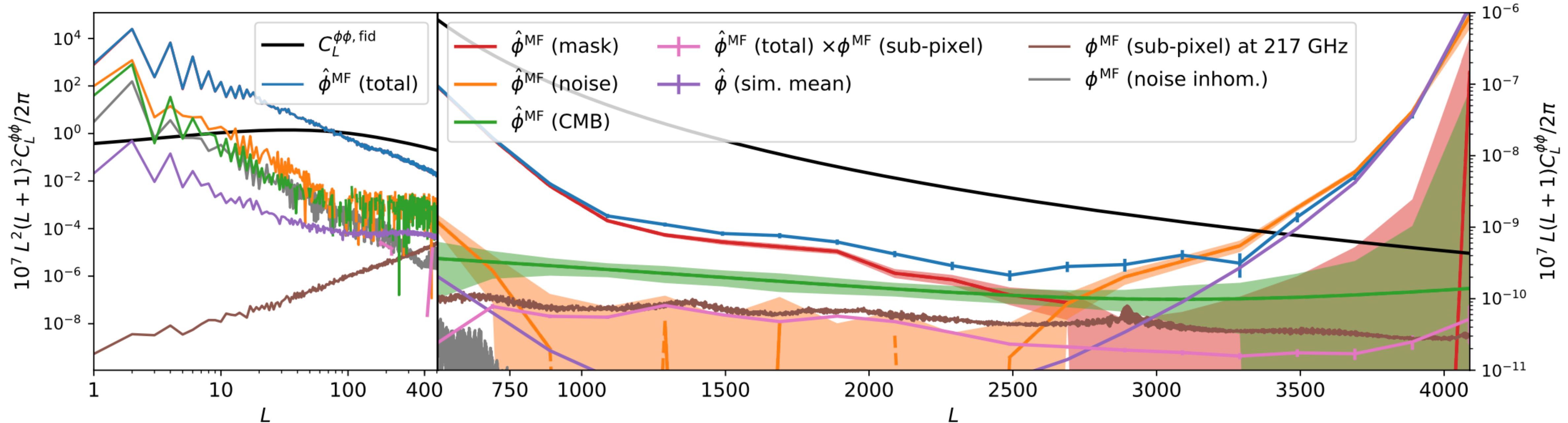
Add then a prior and search for the maximum a posteriori point. The rest are implementation details.

Mean-fields

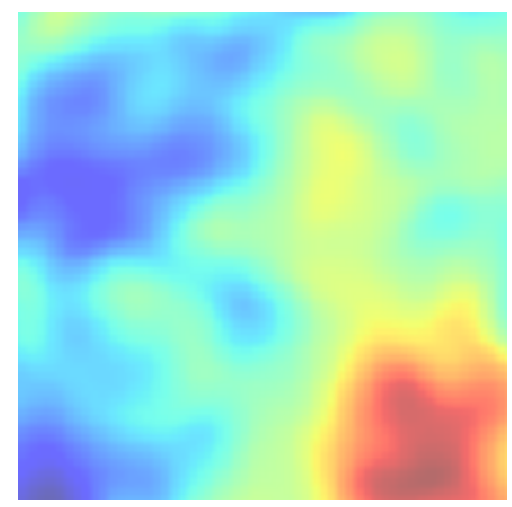
Some ordinary-QE mean-fields:



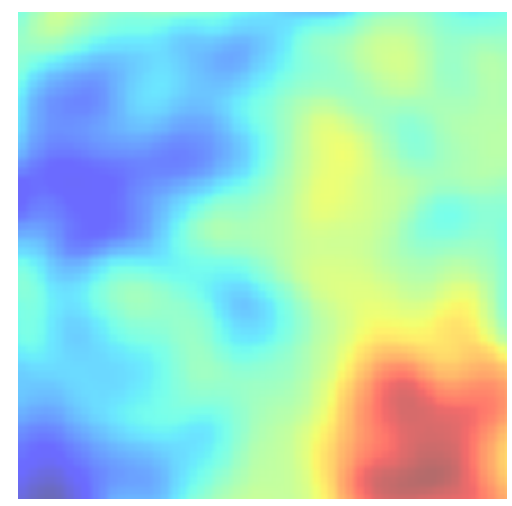
(Here Planck 2018 paper (temperature dominated))



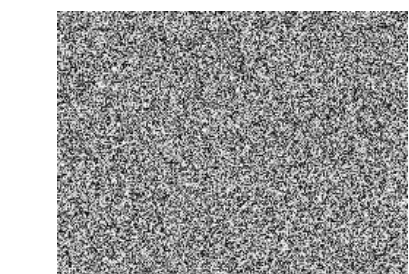
Delensed-noise mean-field



unlensed sky
(undistorted)

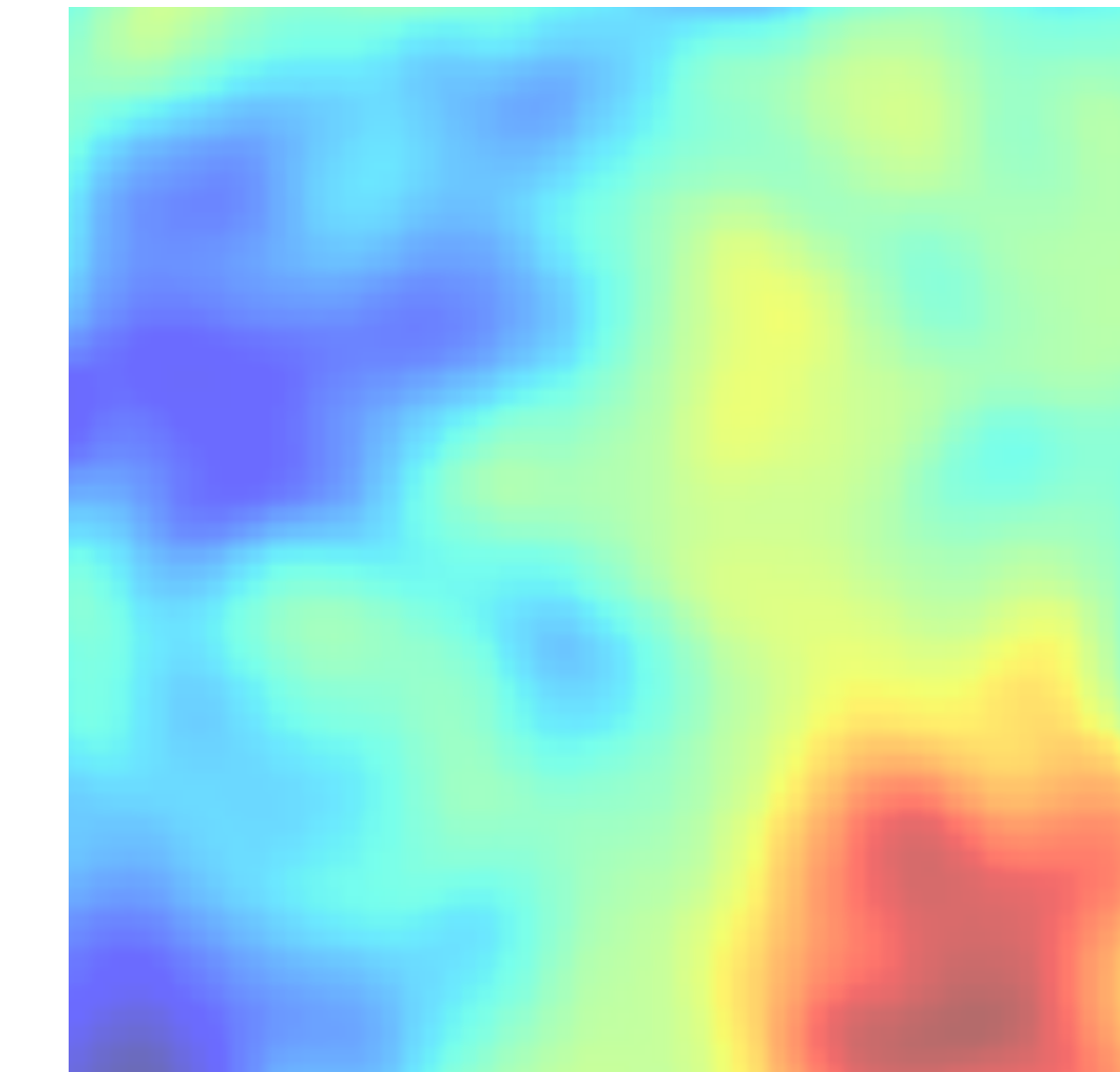


delensed signal
(undistorted)

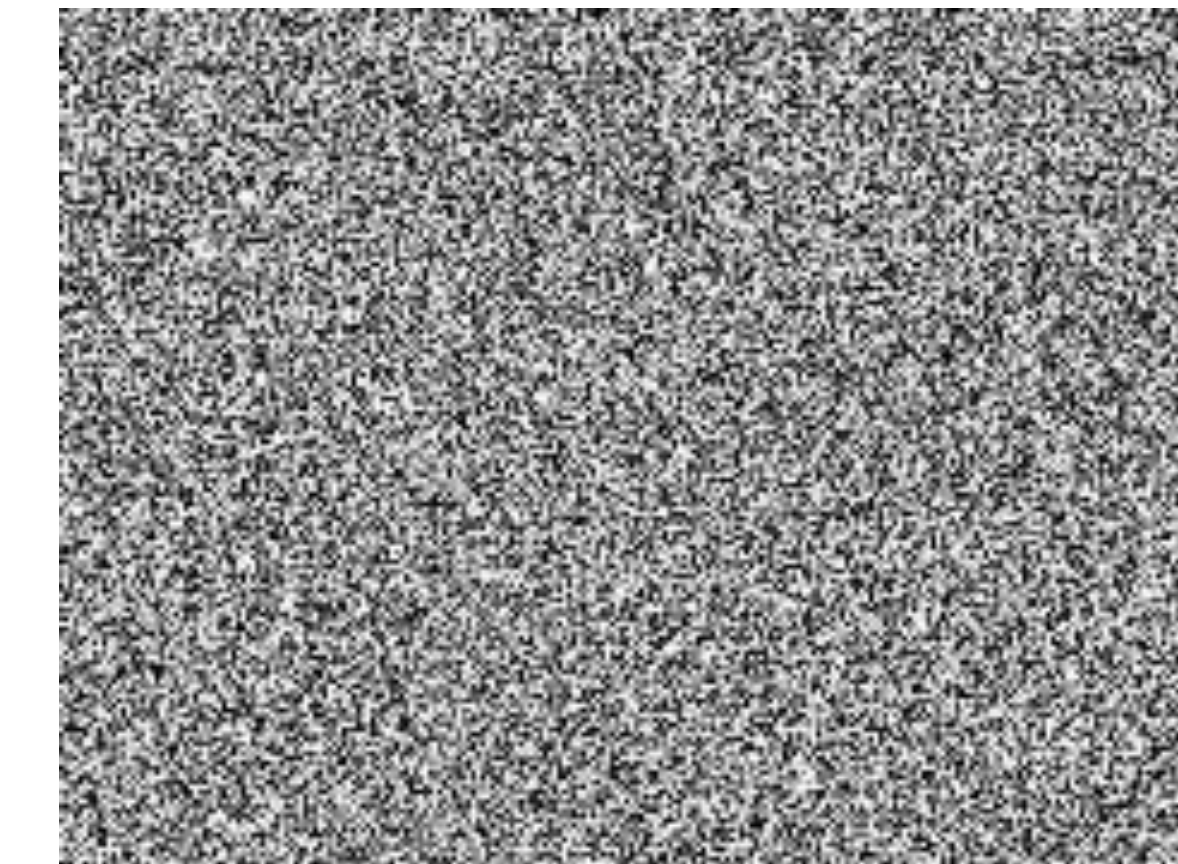


delensed noise
(distorted)

$$\kappa > 0 \quad \text{lensing}$$



observed sky
(distorted)



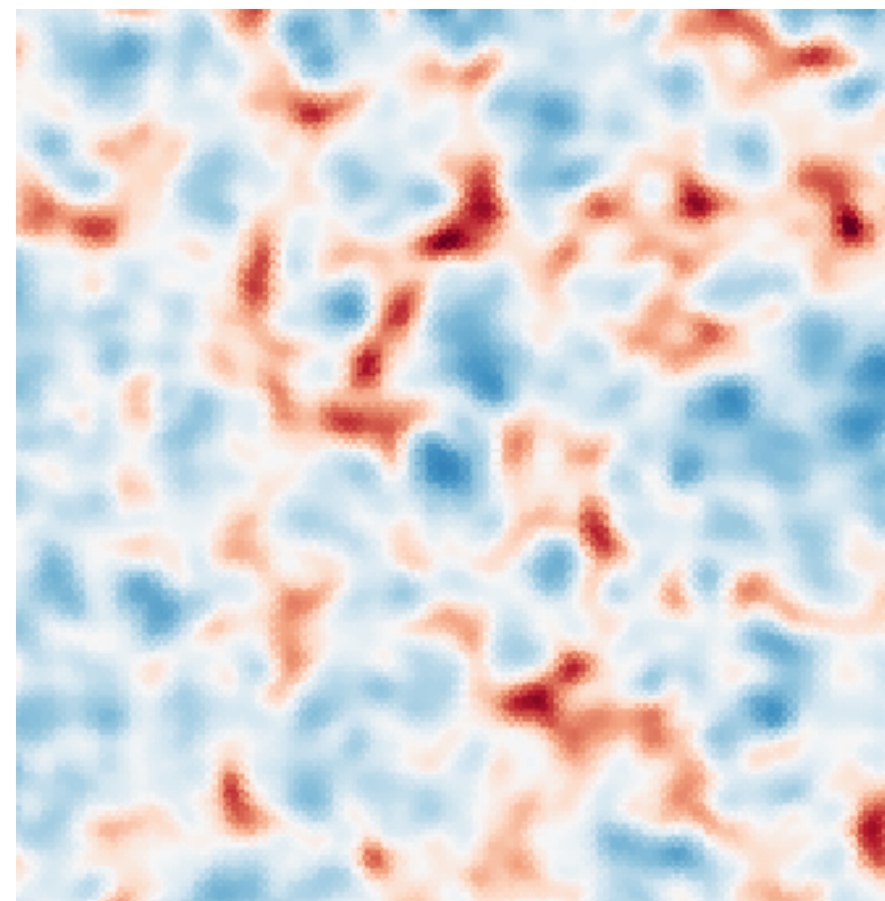
data noise
(possibly undistorted)

Delensed noise mean-field

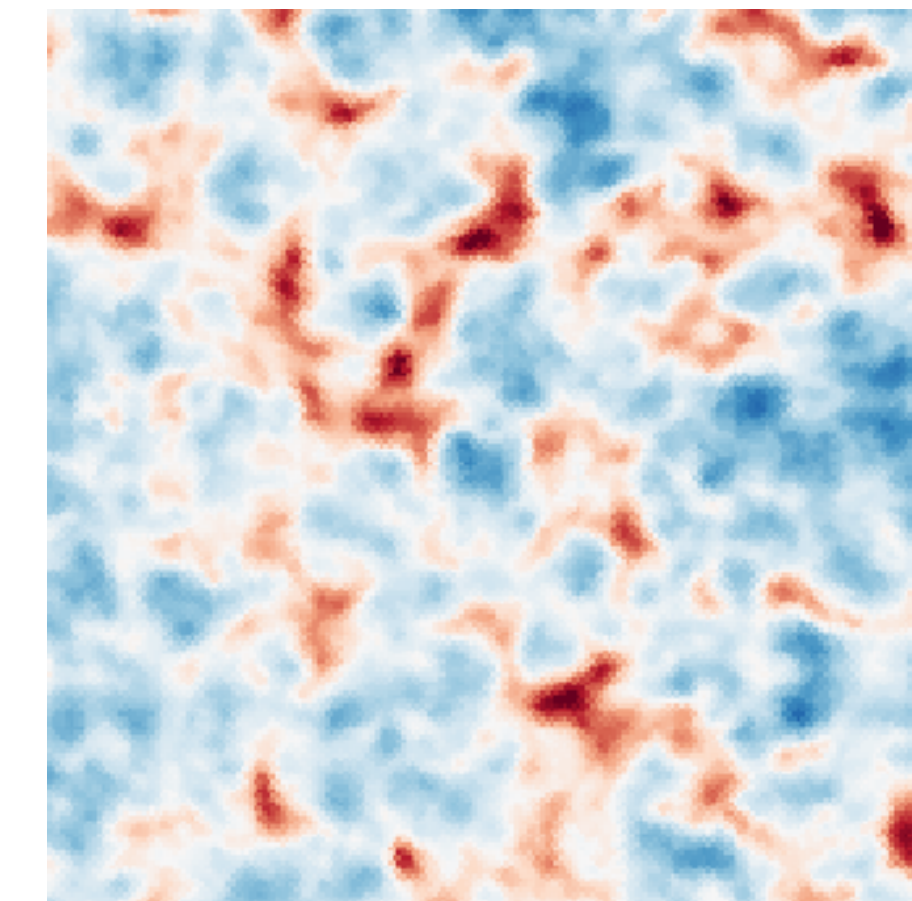
Temperature mean-field linear response $g_{LM}^{\text{MF}} \sim \mathcal{R}_L^{\text{MF}} \kappa_{LM}$

$$\mathcal{R}_L^{\text{MF}} \sim \frac{1}{2} \sum_{\ell} \left(\frac{2\ell + 1}{4\pi} \right) W_{\ell} (1 - W_{\ell}) \times \left[\frac{d \ln \ell^2 C_{\ell}^{\text{del}}}{d \ln \ell} \frac{d \ln \ell^2 N_{\ell}}{d \ln \ell} + \frac{1}{2} \Gamma_L^2 \frac{d \ln C_{\ell}^{\text{del}}}{d \ln \ell} \frac{d \ln N_{\ell}}{d \ln \ell} \right]$$

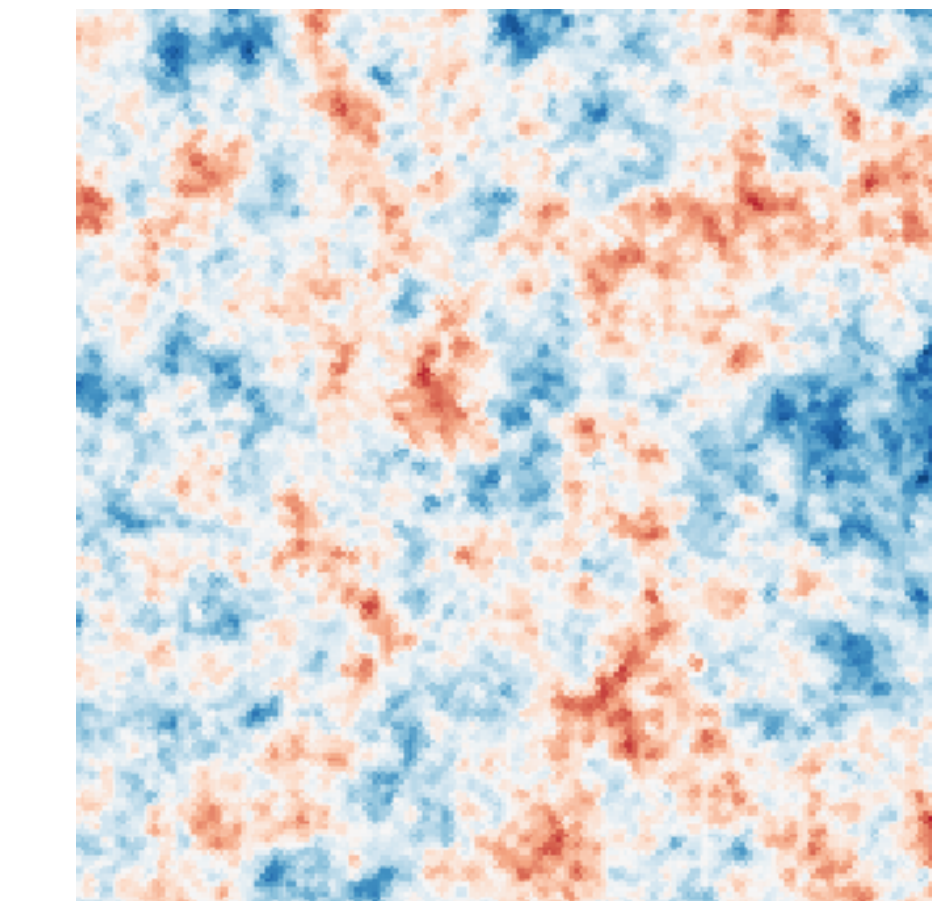
Strong in temperature (15% effect on lensing map in cross-correlation on large scales).
Polarization is mostly protected (no strong EB asymmetry in the noise)



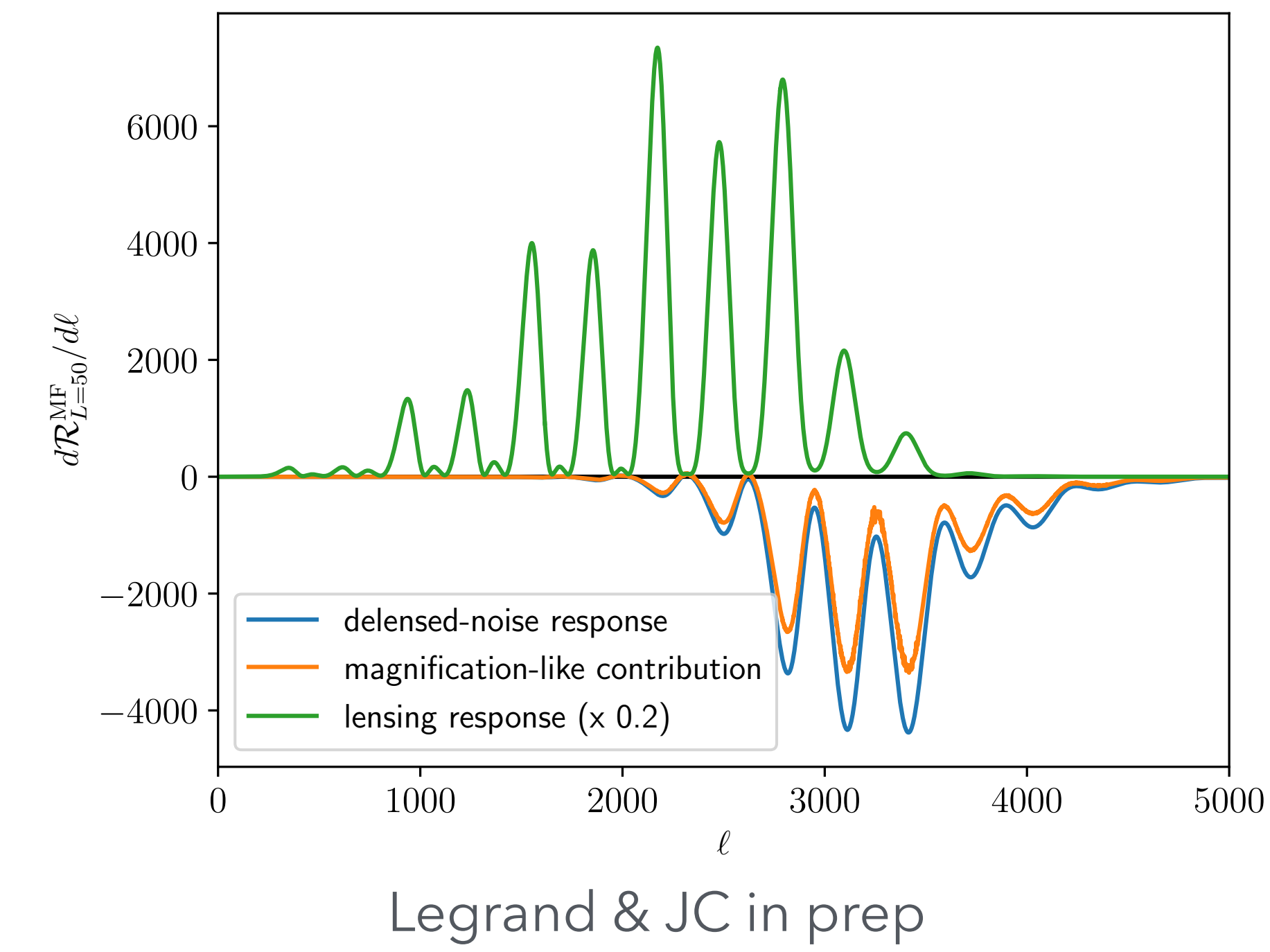
g^{MF} (prediction)



\hat{g}^{MF} (Monte-Carlos)



κ



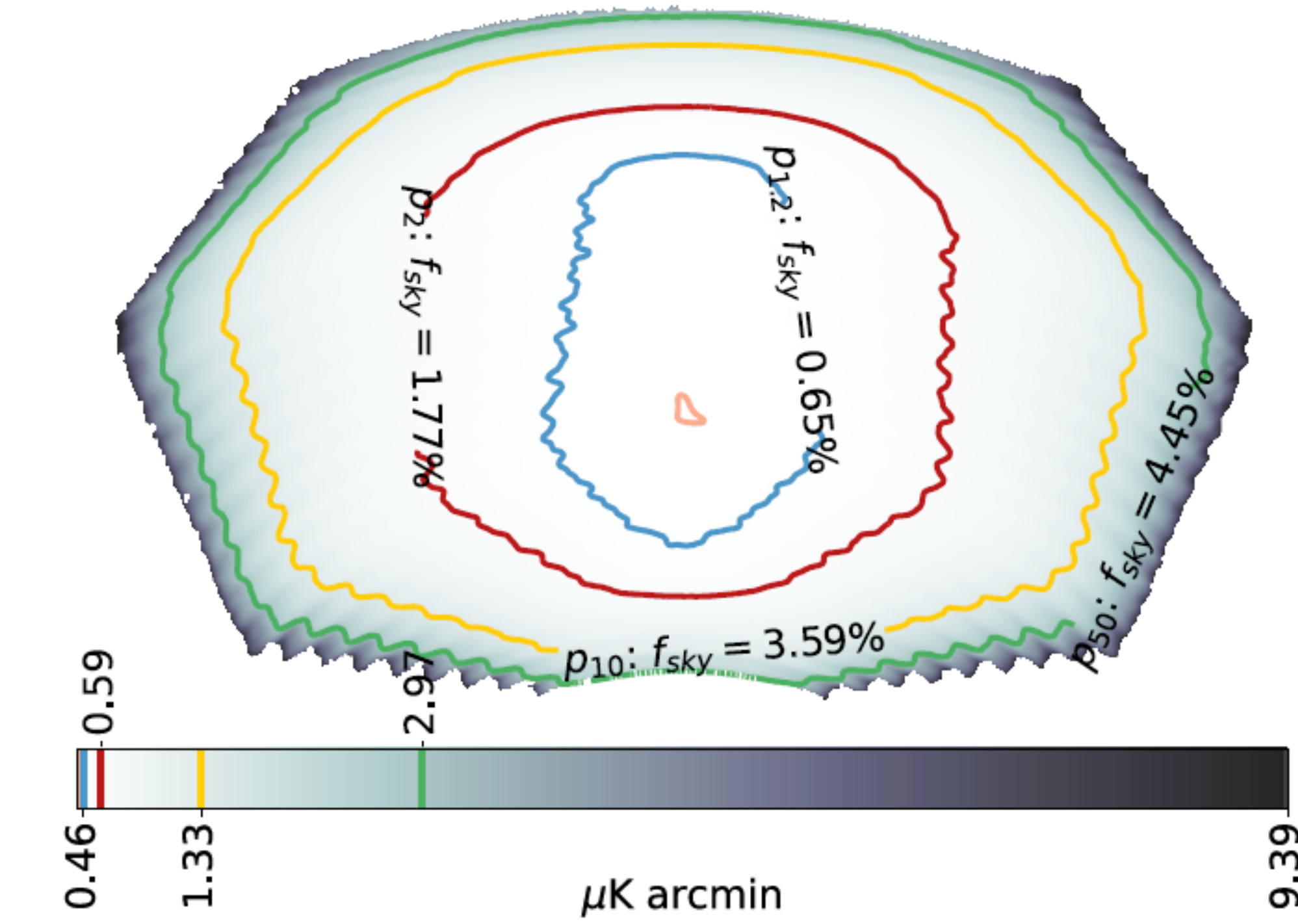
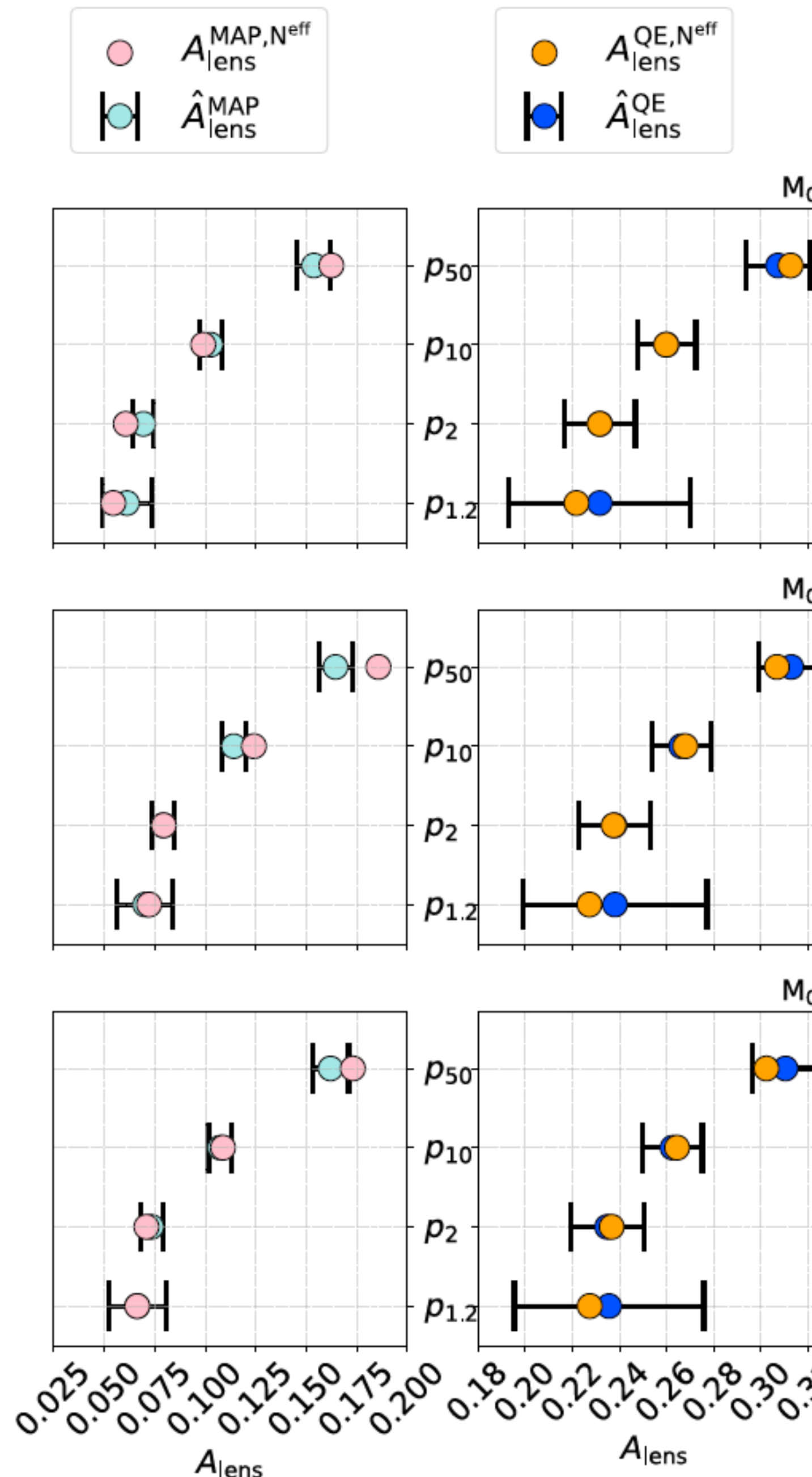
Legrand & JC in prep

Belkner et al 2024 (CMB-S4 delensing paper) gives a detailed description of the method together with a « complete » r-inference pipeline from CMB-S4 LAT and SAT maps at the South Pole inclusive of 95% delensing

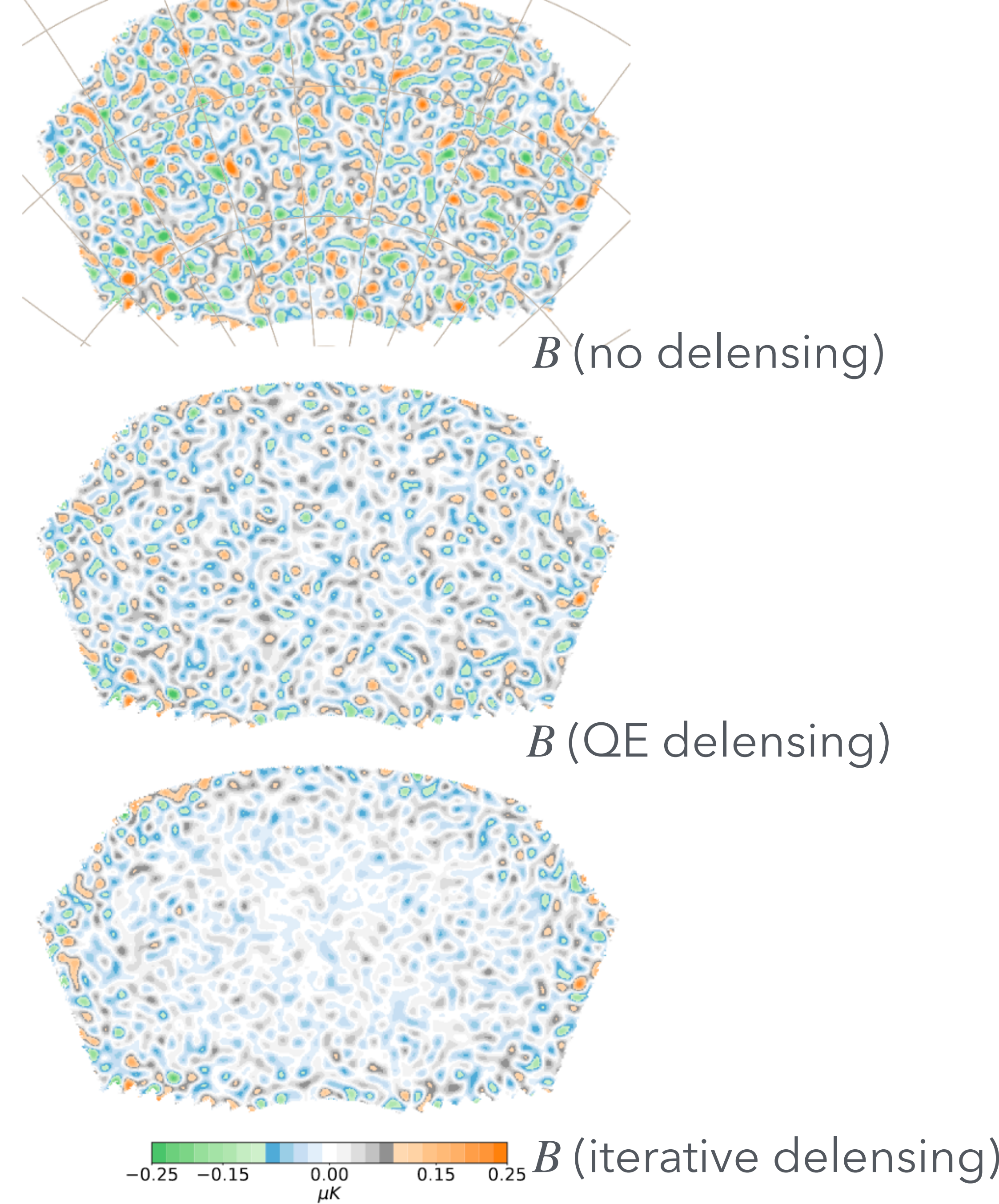
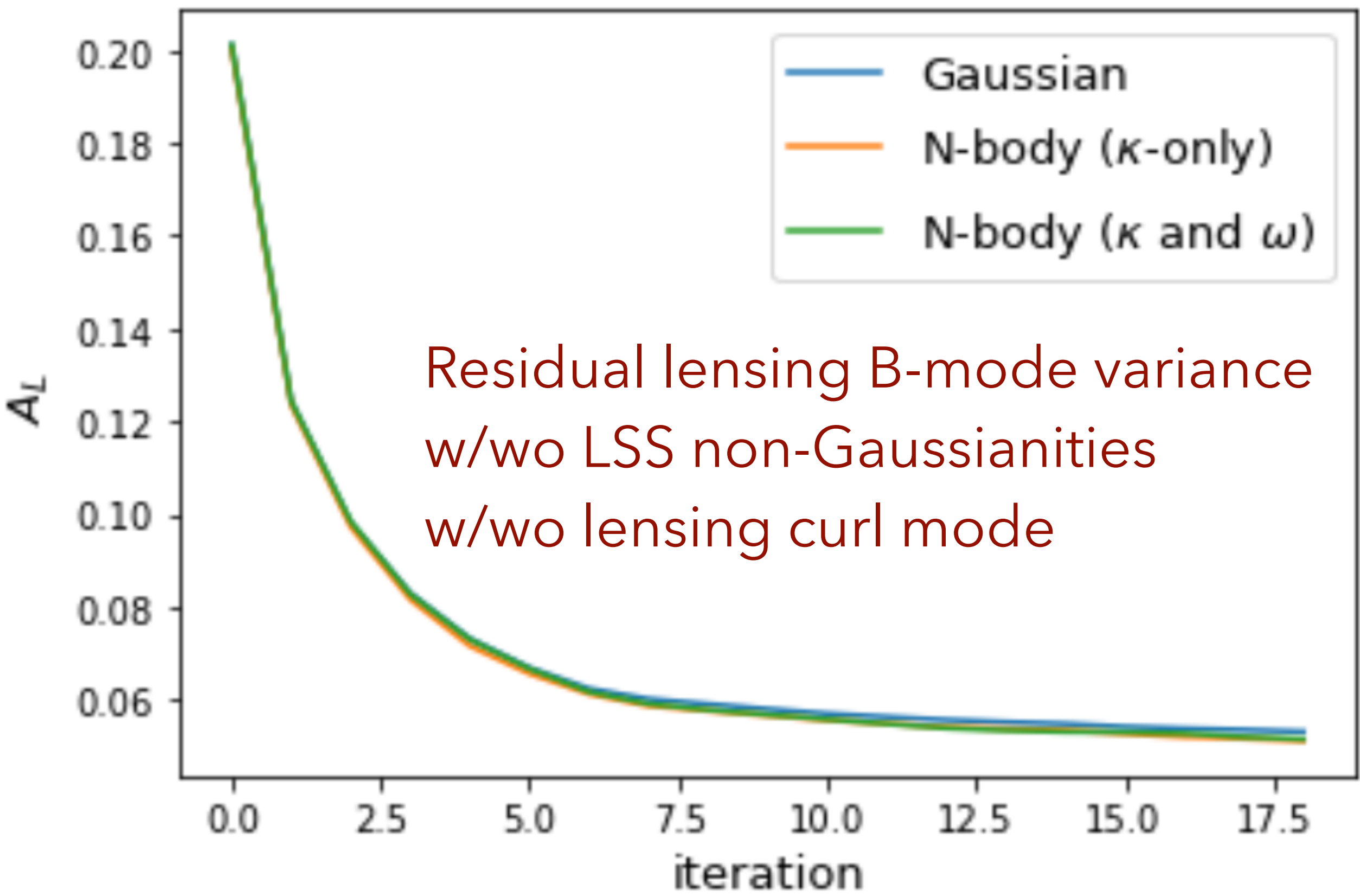
Challenges / tests

- Galactic foregrounds and foregrounds non-Gaussianities. Mostly low-ell issue, so OK
- Mean-fields Low-ell issue, so OK
- non-Gaussianity of lensing field.
(Also Darwish et al 2024) Weak at $L \sim 500$ so OK
- Internal delensing biases We dont use $\ell < 200$ in B
- Impact of lensing curl mode Curl is very small, essentially no impact
- Computational cost. Led to massive improvements

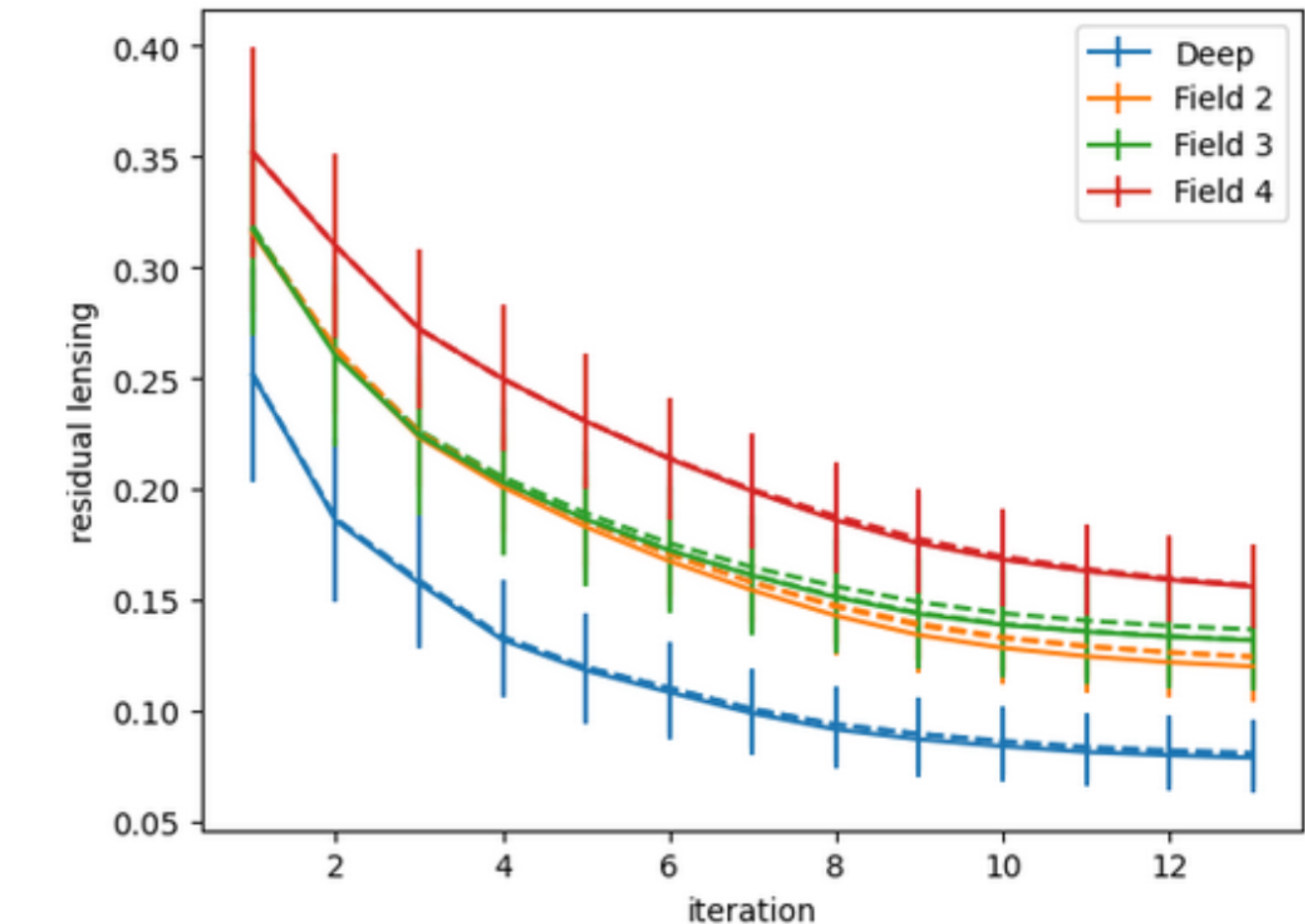
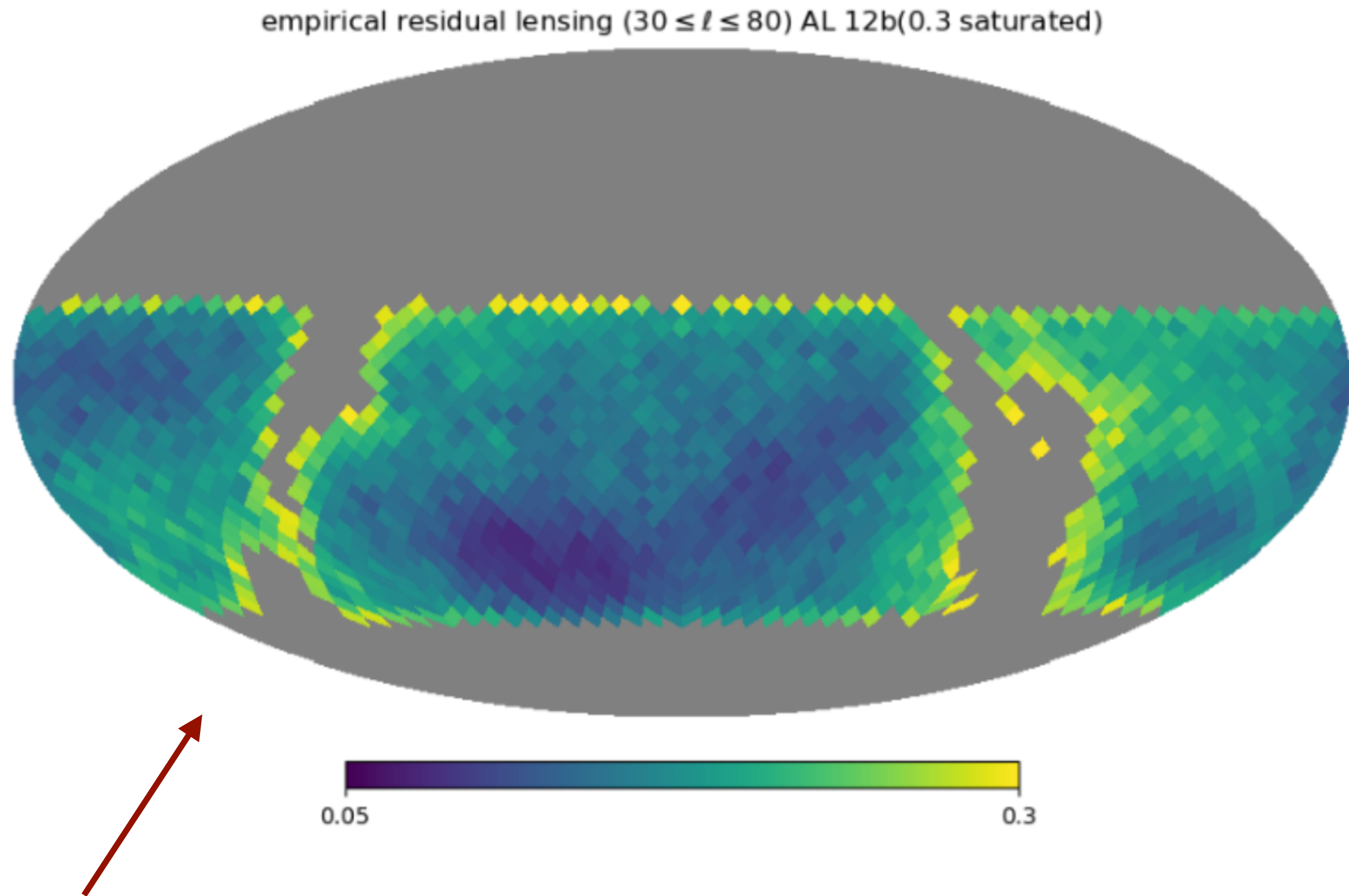
CMB-S4 from South Pole One lesson is that naive predictions for MAP are in fact very accurate



(Belkner et al 2024, CMB-S4 delensing paper)



CMB-S4 from Chile: MAP also works nicely for wider sky coverage



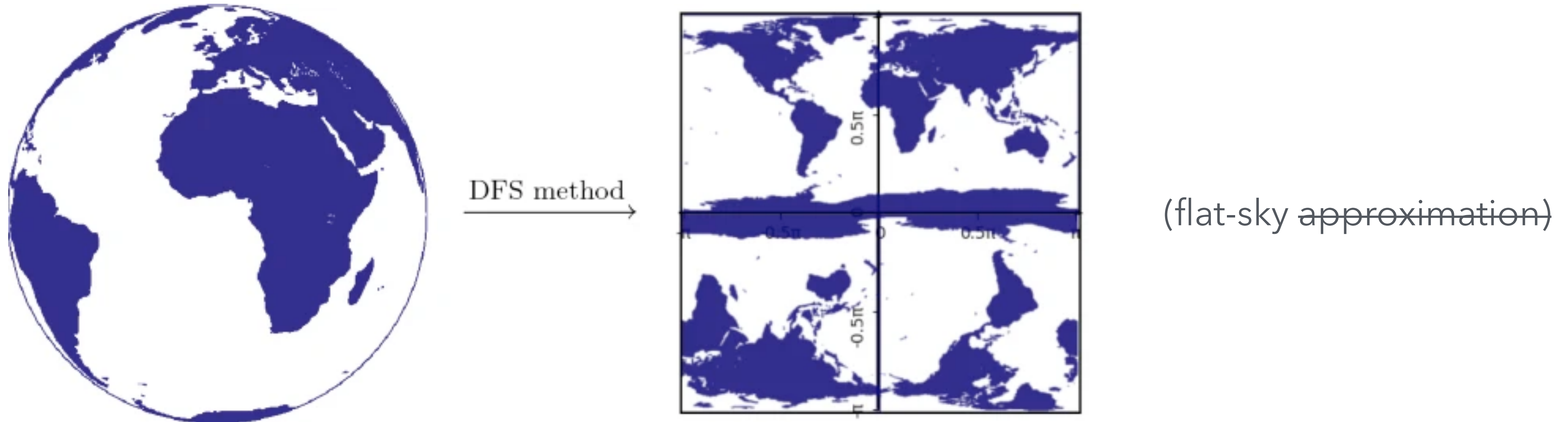
Residual B-lensing variance from 100 reconstructions from NILC-cleaned LAT maps

For a similar hardware configuration:

- Planck PR3 lensing took ~40 minutes to process 100 sims and more for PR4
- This CMB-S4 deep configuration takes ~45 minutes to process 100 sims (5 nodes hours for 100 sims)

Doubled Fourier sphere method

(Basak et al 2008, Reinecke, Belkner & JC 2023)



→ can use optimised accurate modern non-uniform FFT techniques

(Reinecke, Belkner & JC 2023 (CPU), Belkner et al 2024 (GPU). Lenspyx / DUCC)

e.g. 10^8 arbitrary points in 3 sec on laptop

This removes requirement of isolatitudes pixelizations

For example can do catalog-based Cls:

Baleato & White 2023 Wolz, Alonso, Nicola 2024

Summary

MAP lensing reconstruction

- Works in curved-sky geometry and semi-realistic conditions with increase in SNR just as expected
- may be used for delensing, spectrum reconstruction, cluster lensing, x-correlations...
- was tested down to CMB-S4 deep noise levels and in various configurations (for $\ell_{\text{CMB}} \leq 5000$), also including intensity.
- Achieve the CMB-S4 main target on primordial gravitational waves

Thanks!